Article

Current Biology

Vestigial organs alter fossil placements in an ancient group of terrestrial chelicerates

Highlights

- Neuroanatomical and molecular characterization of eye development in daddy-longlegs
- A living daddy-longlegs possesses six eyes, including two vestigial pairs
- Innervation patterns to the brain reflect chelicerate ancestral architecture
- Lateral eyes in living harvestmen change phylogenetic position of four-eyed fossils

Authors

Guilherme Gainett,
Benjamin C. Klementz,
Pola Blaszczyk, ..., Rodrigo Willemart,
Efrat Gavish-Regev,
Prashant P. Sharma

Correspondence

guilherme.gainett@childrens.harvard.edu

In brief

Gainett et al. report that living daddy-longlegs, previously thought to have only two eyes, have additional vestigial eyes only seen in four-eyed fossil relatives. This discovery changes the phylogenetic position of the fossils and pushes back age estimates of this ancient group. These findings underscore the role of vestigial organs in evolution.

Gainett et al., 2024, Current Biology *34*, 1258–1270
March 25, 2024
https://doi.org/10.1016/j.cub.2024.02.011

CellPress

CellPress

Current Biology

Article

Vestigial organs alter fossil placements in an ancient group of terrestrial chelicerates

Guilherme Gainett,[1,2,3,6,7,*] Benjamin C. Klementz,[1] Pola Blaszczyk,[1] Emily V.W. Setton,[1] Gabriel P. Murayama,[5] Rodrigo Willemart,[5] Efrat Gavish-Regev,[4] and Prashant P. Sharma[1]

[1]Department of Integrative Biology, University of Wisconsin-Madison, Madison, WI 53706, USA
[2]Department of Pathology, Boston Children's Hospital, Boston, MA 02115, USA
[3]Department of Systems Biology, Harvard Medical School, Boston, MA 02115, USA
[4]The National Natural History Collections, The Hebrew University of Jerusalem, Edmond J. Safra Campus, Givat Ram, Jerusalem 9190401, Israel
[5]Laboratório de Ecologia Sensorial e Comportamento de Artrópodes, Escola de Artes, Ciências e Humanidades, Universidade de São Paulo, Rua Arlindo Béttio, 1000, Ermelino Matarazzo, São Paulo, SP 03828-000, Brazil
[6]X (formerly Twitter): @Gainetting
[7]Lead contact
*Correspondence: guilherme.gainett@childrens.harvard.edu
https://doi.org/10.1016/j.cub.2024.02.011

SUMMARY

Vestigial organs provide a link between ancient and modern traits and therefore have great potential to resolve the phylogeny of contentious fossils that bear features not seen in extant species. Here we show that extant daddy-longlegs (Arachnida, Opiliones), a group once thought to possess only one pair of eyes, in fact additionally retain a pair of vestigial median eyes and a pair of vestigial lateral eyes. Neuroanatomical gene expression surveys of eye-patterning transcription factors, opsins, and other structural proteins in the daddy-longlegs *Phalangium opilio* show that the vestigial median and lateral eyes innervate regions of the brain positionally homologous to the median and lateral eye neuropils, respectively, of chelicerate groups like spiders and horseshoe crabs. Gene silencing of *eyes absent* shows that the vestigial eyes are under the control of the retinal determination gene network. Gene silencing of *dachshund* disrupts the lateral eyes, but not the median eyes, paralleling loss-of-function phenotypes in insect models. The existence of lateral eyes in extant daddy-longlegs bears upon the placement of the oldest harvestmen fossils, a putative stem group that possessed both a pair of median eyes and a pair of lateral eyes. Phylogenetic analysis of harvestman relationships with an updated understanding of lateral eye incidence resolved the four-eyed fossil group as a member of the extant daddy-longlegs suborder, which in turn resulted in older estimated ages of harvestman diversification. This work underscores that developmental vestiges in extant taxa can influence our understanding of character evolution, placement of fossils, and inference of divergence times.

INTRODUCTION

Vestigial organs have long fascinated evolutionary biologists for their potential to clarify common ancestry and macroevolutionary processes.[1–3] The value of vestigial traits in evolutionary theory is that they can bridge gaps in transformation series of morphological structures in paleontological datasets with their modern counterparts in extant taxa when complex organs become less elaborate or non-functional over time.[4–6] However, the empirical importance of vestigial organs for inferring the phylogenetic position of contentious fossils remains poorly documented. For many taxa, the phylogenetic position of fossils often relies on a small number of characters, and the absence of comparable morphologies in extant taxa may convolute the correct placement of fossils in the Tree of Life.[7–10]

One organ system whose evolutionary history is often complex is the arthropod visual system. Arthropod eyes are diverse in form and function and have undergone repeated losses and gains across the phylum.[11] Chelicerates (sea spiders, horseshoe crabs, and other arachnids) have two types of visual systems, the median eyes (principal eyes) and the lateral eyes (secondary eyes), which differ in their mode of embryogenesis, acuity, and innervation to the brain.[12,13] Evidence from position, gene expression, and anatomy suggests that the median and lateral eyes of chelicerates are homologous, respectively, to the ocelli and the compound eyes of pancrustaceans.[14–16] However, within Chelicerata, the number of eyes and the degree of reduction of their visual systems vary extensively.[17]

In the order Opiliones, commonly known as harvestmen or daddy-longlegs, extant species have a maximum of one pair of single-lens camera-type eyes.[18] In Phalangida (which includes daddy-longlegs [Eupnoi]), a pair of median eyes is placed on a dorsal body protrusion, the ocularium (Figure 1A).[18,19] In Cyphophthalmi (mite harvestmen), most groups lack evidence of eyes, but species in two families retain a pair of simplified eyes associated with dorsolateral protrusions of the body, called

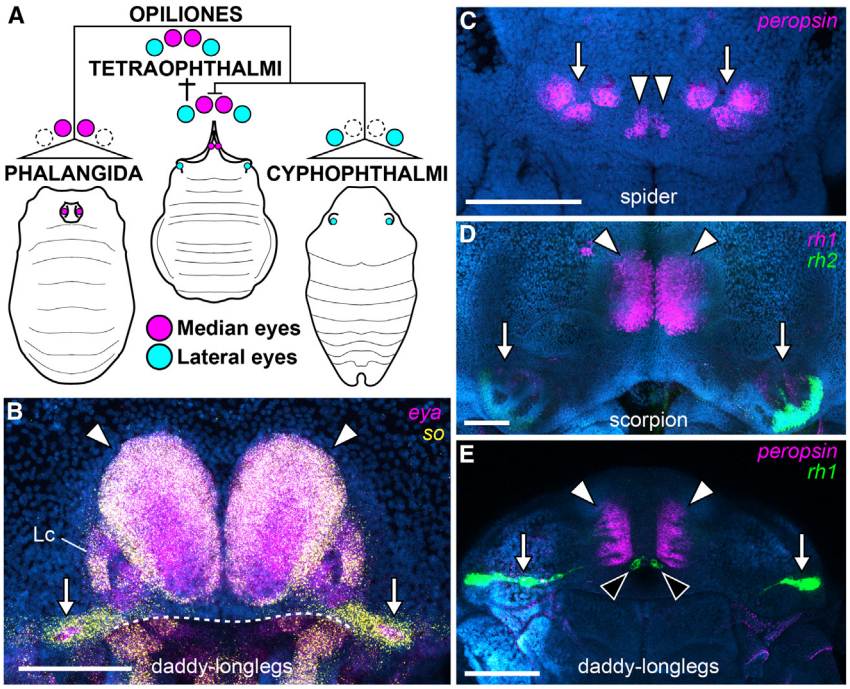

Figure 1. The paradigm of harvestman eye evolution and presence of rudimentary eyes in embryos of the daddy-longlegs *P. opilio* (evidence from molecular markers)

(A) Mite harvestmen (Cyphophthalmi) have one pair of lateral eyes, in contrast to their sister group, Phalangida, which were thought to have one pair of median eyes. The fossil suborder Tetraophthalmi has both pairs of eyes and was previously recovered as a stem-group Cyphophthalmi.[21]

(B) Developing eyes in *P. opilio*, showing mRNA expression of *eya* in magenta and *so* in yellow (frontal view).

(C) Head of a spider embryo (frontal view). mRNA *peropsin* expression in magenta.

(D) Head of a scorpion embryo (frontal view). mRNA expression of *rh*1 and *rh2* paralogs is shown in magenta and green.

(E) Head of a *P. opilio* daddy-longlegs embryo (frontal view). mRNA *peropsin* expression (magenta) and mRNA *rh1* expression (green). Nuclei in blue (Hoechst).

White arrow, lateral cells; black arrowhead, median cells; white arrowhead, median eyes. Lc, lateral brain center. Scale bars, 100 μm.

ozophores (Figure 1A).[20] Recently, a putative stem-group fossil harvestman, *Hastocularis argus*, was discovered that exhibits two pairs of eyes, with one pair associated with an ocularium and the other with the ozophores.[21] This condition is not seen in any extant harvestman and implies that the common ancestor of Opiliones possessed both visual systems, that Cyphophthalmi eyes are true lateral eyes (associated with ozophores), and that Phalangida eyes are true median eyes (associated with the ocularium) (Figure 1A). The four-eyed fossil *H. argus* and the oldest known Rhynie Chert Opiliones fossil, *Eophalangium sheari*, were previously recovered in a clade (Tetraophthalmi) as stem-group mite harvestmen in a total-evidence analysis (Figure 1A),[21,22] but this placement is potentially unstable for three reasons: (1) it renders the evolution of multiple characters non-parsimonious (supporting text at Dryad: 10.5061/dryad.m905qfv6q); (2) the molecular data were limited to five genes; and (3) the morphological dataset was coded for a small number of extant terminals, none of which exhibited the four-eyed condition found in the fossils.

Comparatively little is known about the patterning of chelicerate eyes with regard to developmental genetics, in contrast to better-studied insect models.[15,23] Previous work on chelicerate eye development has emphasized embryonic gene expression in a horseshoe crab and multiple species of spiders.[24–29] Functional data on arachnid eye development were previously restricted to a single investigation of a spider homolog of *sine oculis*, a member of a conserved gene regulatory network underlying eye patterning across Bilateria.[29] As part of a comparative investigation to elucidate the molecular basis of eye development across chelicerates, we explored eye development in the daddy-longlegs *Phalangium opilio* (an exemplar of Phalangida; Figure 1A). During this investigation, we established the unexpected presence of previously unreported rudimentary median and lateral eyes. This finding prompted us to assess the influence of these rudimentary eyes on the phylogenetic position of four-eyed fossil harvestmen and reevaluate scenarios of eye evolution in Opiliones and Chelicerata.

RESULTS AND DISCUSSION

An extant daddy-longlegs has multiple rudimentary eye pairs

The retinal determination network (RDN) includes important genes conserved across bilaterians in initiating and patterning photoreceptive structures, such as *Pax6*, *eyes absent* (*eya*), and *sine oculis* (*so; Six1*).[30,31] To investigate eye development in the harvestman *P. opilio*, we described the expression patterns of eight genes (supporting text at Dryad: 10.5061/dryad.m905qfv6q; Figures 1 and S1–S4) that are known to be important for eye morphogenesis and photoreceptor specification in the ocelli and compound eyes of the fruit fly *Drosophila melanogaster*,[30] and whose homologs exhibit expression in the median and lateral eyes of other chelicerates, such as spiders.[25,26]

The median eyes of the harvestman *P. opilio* develop as two large bilateral eye folds[32] that progress anteriorly over the neuroectoderm as part of a morphogenetic process that will contribute to the formation of the anterior portion of the prosomal shield[33] (Figures 1B and 2A–2E; supporting text at Dryad: 10.5061/dryad.m905qfv6q). When fully folded, the eye is a multilayered tissue above the developing brain[32] (Figures 2F–2M'; see Figure 2J' for orientation). The eye has two distinct regions in the frontal view, a mesal compartment and an ectal compartment (Figure 2E). All eight genes (*eyes absent* [*Po-eya*], *sine oculis* [*Po-so*], *Po-Optix*, *dachshund* [*Po-dac*], *orthodenticle* [*Po-otd*], *Pax6* paralogs [*Po-Pax6a* and *Po-Pax6b*], and *Po-Pax2*) are

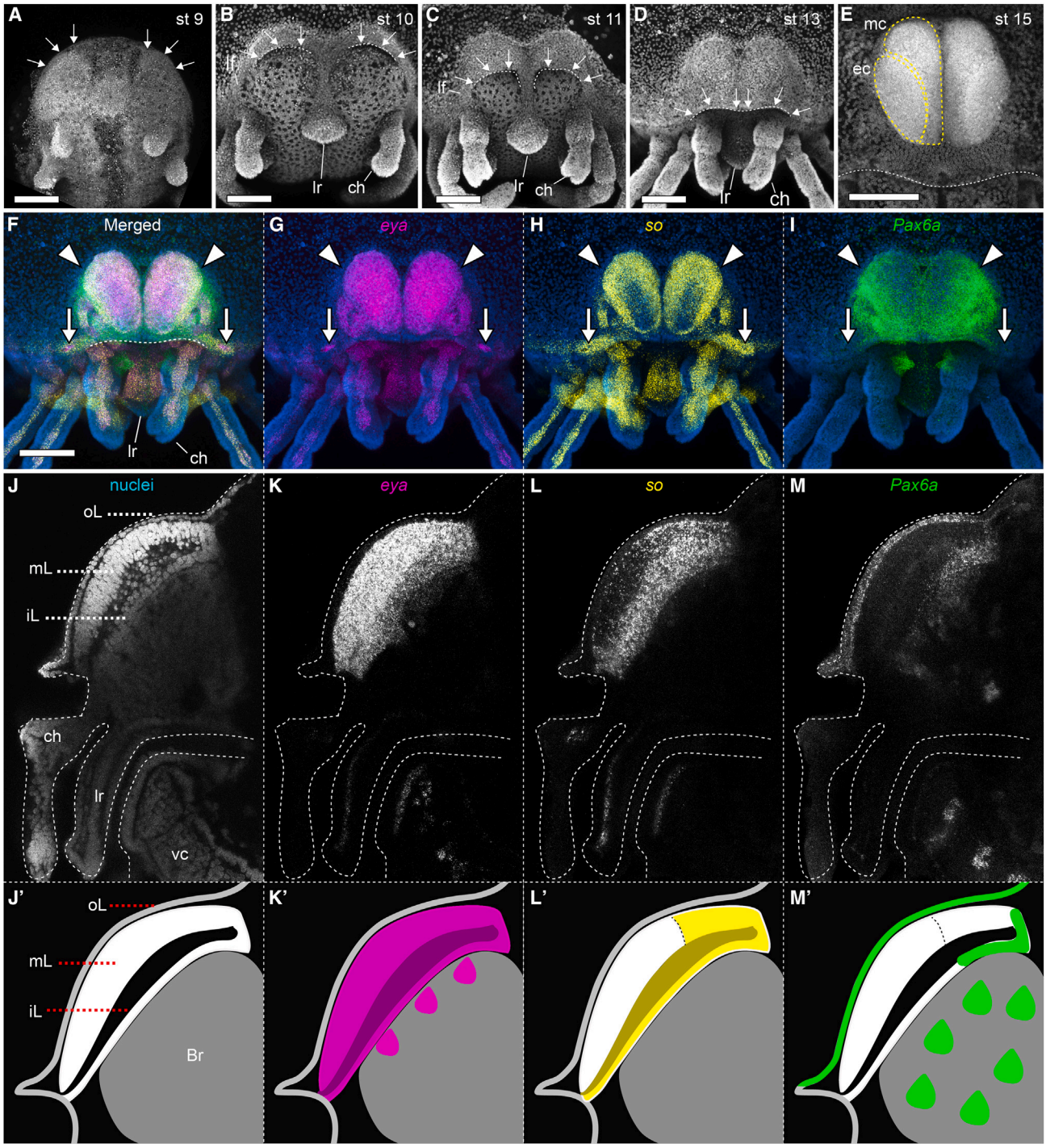

Figure 2. Eye development in the daddy-longlegs *P. opilio*

(A–E) Progression of head development in a series of embryonic stages (Hoechst staining; maximum projection). Arrows mark the anterior margin of the head, which shifts anteriorly to cover the neurogenic ectoderm. Embryos in (A)–(D) are also shown in Figure S1 (atlas).

(F–I) Stage 13 embryo, triple labeled with *eya* (magenta), *so* (yellow), and *Pax6a* (green) expression (maximum projection). Nuclei in blue (Hoechst). The same embryo is shown in Figures 1B and S1 (atlas).

(J–M) Single optical slice of the developing median eye (stage 13), triple marked with *eya* (magenta) (K), *so* (yellow) (L), and *Pax6a* (green) (M) expression. Note that *Pax6a* is mostly restricted to the outer layer (lentigenic layer) of the median eyes, while *eya* and *so* are ubiquitous in the median and inner layers. (J′–M′) Schematic representation of the morphology and expression patterns in the eye cross-section.

(legend continued on next page)

expressed in parts of the developing eye tissue and brain at some stage of development analyzed here (stages 8–16) (Figures S1–S3). Eye layers express different combinations of genes. For instance, while *Po-eya* is ubiquitously expressed in all three layers, *Po-so* is concentrated on the dorsal part of the medium retinal layer and in the inner retinal layer, whereas *Po-Pax6a* is restricted to the outer lentigenic layer (Figures 2J–2M′). *Po-Optix* is expressed in parts of the eye fold, developing brain, and labrum, as well as the mesal compartment of the multi-layered eye (Figures S1H–S1M). *Po-Pax6a* (Figures 2I, 2M, 2M', and S1A–S1G) and *Po-Pax6b* (Figure S2) are mainly expressed in the neural tissue during eye folding but are also weakly expressed in parts of the eye folds. *Po-eya*, *Po-so*, *Po-otd*, *Po-dac*, and *Po-Pax2* expression overlaps in large areas of the median eye tissue throughout eye fold progression and in the multi-layered eye (Figures 2F–2H and S1–S3), with the exception that *Po-dac* expression becomes restricted to the outer layer of the eye in late stages (stage 15 onward) (Figure S1M).

In sum, ubiquitous spatial and temporal expression of *Po-eya* and *Po-so* (Figures 1B and S1A–S1G), as well as of *Po-otd* (Figure S2) and *Po-Pax2* (Figures S3A–S3E), is associated with all phases of median eye development, suggesting a pivotal role for these genes in the establishment and differentiation of the median eyes of *P. opilio*.

Beyond the median eyes, expression of *Po-eya* and *Po-Pax2* occurs within a broader domain of *Po-so* expression on the anterolateral margin of the head, adjacent to the lateral furrow (Figures 1B, S1A–S1G, and S3A–S3E). This region corresponds to the site of lateral optic neuropil and lateral eye development in arachnids with lateral eyes.[25,26,34] These *Po-eya* and *Po-Pax2* domains temporally precede foci of *Po-otd* expression, which is co-expressed with *Po-eya* in these cells during the stages investigated (Figure S2). In addition, *Po-dac* is broadly expressed in this lateral territory (Figures S1H–S1M). All eight genes studied are expressed in parts of the developing lateral region of the brain (hereafter, lateral brain center), in most cases as a discreet C-shaped outline (Figures 1B, 2F–2H, S1F, S1K, S1L, and S3A–S3E).

The seemingly vestigial co-expression of the eye-patterning genes where lateral eyes normally form in arachnids prompted us to investigate whether *P. opilio* develops rudimentary eyes. We investigated the expression of opsin-encoding genes, as opsins are conserved proteins upstream of the photoreceptive cascade in photoreceptive organs across Metazoa.[35] Long-wavelength-sensitive (LWS) r-opsins are known to be canonical visual opsins in arachnids,[36] whereas peropsin has previously been detected in the retina of spiders.[37] As a point of comparison, we first visualized embryonic expression of LWS r-opsins and a peropsin in a spider (*Parasteatoda tepidariorum*) and a scorpion (*Centruroides sculpturatus*), two arachnid groups that possess both median and lateral eyes. In the spider *P. tepidariorum*, peropsin mRNA (*Pt-peropsin*) is expressed in the median and lateral eyes of late embryos (stage 14), but LWS r-opsin mRNA (*Pt-rh1* and *Pt-rh2*) is not embryonically expressed in the eyes (Figure 1C). In the scorpion *C. sculpturatus*, peropsin mRNA (*Cs-peropsin*) was not detected in the embryonic eyes, whereas one LWS r-opsin paralog (*Cs-rh1*) is expressed mostly in the median eyes, and a second LWS r-opsin paralog (*Cs-rh2*) is expressed only in the lateral eyes (Figure 1D). These results show that, despite some evolutionary variability, embryonic opsins serve as specific markers for both median and lateral eyes of arachnids.

Eight opsin genes occur in the genome of *P. opilio* (Figure S4). We identified transcripts predicted as three c-opsins (non-visual), a peropsin (*Po-peropsin*), and four r-opsins (*Po-rh1*, *Po-rh3*, *Po-rh7*, and *Po-arthropsin*) (Figure S4). In embryonic stages shortly prior to eye pigment formation (stages 13–14), we detected *Po-peropsin* expression in the median eyes and *Po-rh1* (a LWS r-opsin) in a group of cells in the lateral margin of the head (Figure 1E), co-localizing with *Po-eya* in the lateral cells (Figure 3A). This differential expression of *Po-peropsin* and *Po-rh1* expression between the median eyes and the lateral cells persists until stage 18, when *r-opsin* also becomes expressed in the median eyes (Figure 3B). Unexpectedly, *Po-rh1* is additionally expressed in two small groups of cells anterior to the median eyes (hereafter median cells), which also do not express *Po-peropsin* initially and occur within a *Po-eya* expression domain (Figures 1E, 3A, 3B, and 3I). *Po-rh3* (UV opsin) is expressed in the developing median eyes, lateral cells, and median cells, whereas we did not detect expression of *Po-rh7* and *Po-arthropsin* in this territory throughout embryogenesis (Figure 3E). The opsin-positive lateral cells are also present in post-embryonic stages and adults (Figures 3J–3N).

Visual arrestin (beta-arrestin) proteins are important downstream components of the photoreception cascade,[38] and myosin-III protein (whose encoding gene is a homolog of *D. melanogaster ninaC*) is a photoreceptor-specific marker in the horseshoe crab that is known to localize to the developing larval and adult lateral and median eyes.[39,40] In the genome and transcriptomes of *P. opilio*, we discovered two putative visual arrestins (*Po-arrestin-2* and *Po-arrestin-2-like*) and two myosin-III homologs (*Po-myoIII-1* and *Po-myoIII-2*). Most genes (except *Po-arrestin-2-like*; no expression detected) are expressed in the median eyes and median cells, whereas *Po-arrestin-2* and *Po-myoIII-2* are also expressed in the lateral cells (Figures 3C, 3D, and 3F–3H). The combined expression of an LWS r-opsin, a UV opsin, and downstream photoreceptor-specific genes strongly suggests that the lateral and median cells are photoreceptive. Together with the expression data of RDN genes, these data support the interpretation that both the lateral and median cells are rudimentary eyes.

Median and rudimentary eyes of *P. opilio* are under control of retinal determination genes

To further test the hypothesis that the lateral and median cells are eye homologs, we investigated whether genes patterning all eyes (median and lateral) in other arthropods are necessary for

White arrow, lateral cells; white arrowhead, median eyes. Br, brain; ch, chelicera; ec, ectal compartment of the median eye; lf, lateral furrow; lr, labrum; iL, inner layer of the median eye; mc, mesal compartment of the median eye; mL, median layer of the median eye; oL, outer layer of the median eye; vc, ventral nerve cord. Scale bars, 100 μm.
See also Figures S1–S3.

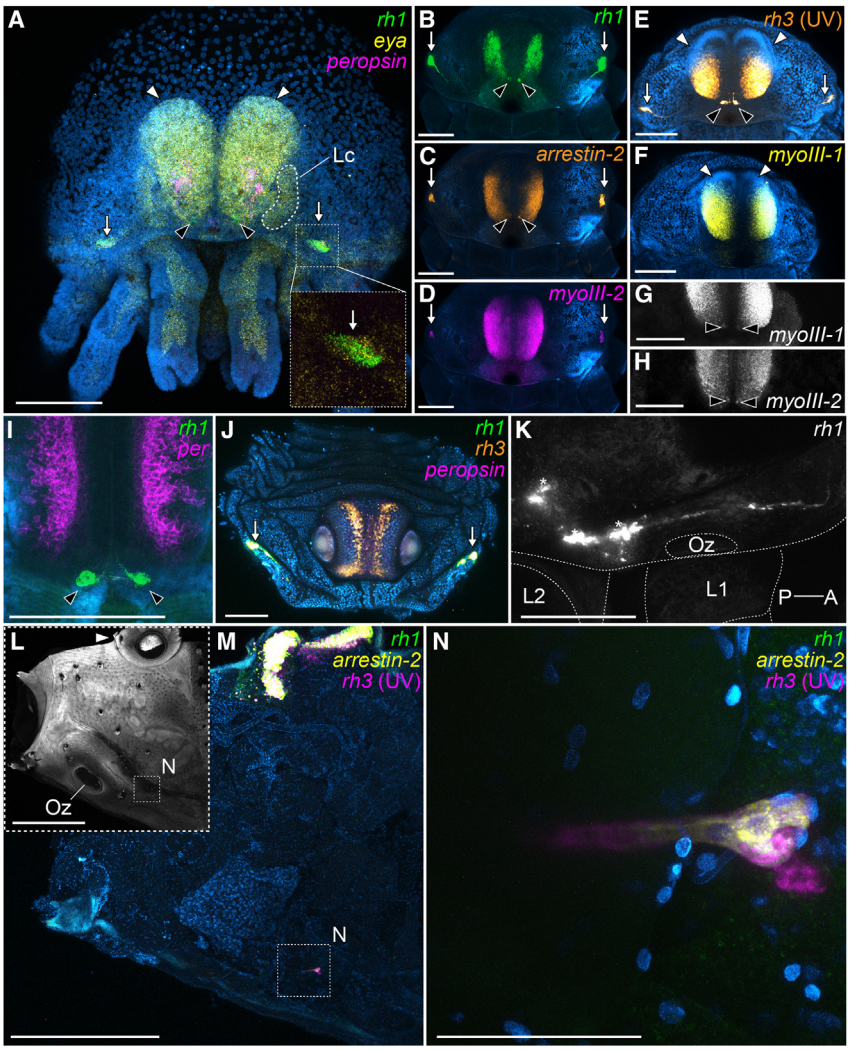

Figure 3. Median cells and lateral cells express photoreception genes

(A) Stage 13 embryo, showing *eya* (yellow) mRNA co-expression with *rh1* (green) mRNA in the median and lateral cells, and *peropsin* (magenta) in the median eyes. Inset: detail of the *eya* and *rh1* expression in the lateral cells.

(B–D) Stage 17 embryo (multiplexed), marked with *rh1* (green) (B), *arrestin-2* (orange) (C), and *myosin III-2* (*myoIII-2*) (magenta) (D) expression. Note that in this stage *rh1* is also expressed in the median eyes.

(E) Stage 17, *rh3* (UV) expression.

(F) Stage 17, *myosin III-1* (*myoIII-1*) expression.

(G) Sub-stack of (F), showing expression of *myoIII-1* in the median cells.

(H) Sub-stack of (D), showing expression of *myoIII-2* in the median cells.

(I) Close-up of *rh1* expression (green) in the median cells and *peropsin* expression (magenta) in the median eyes of a stage 16 embryo.

(J) *rh1* (green), *rh3* (orange), and *peropsin* (magenta) expression in a third instar individual.

(K) Lateral view of the rudimentary lateral eye in a third instar individual. *rh1* expression in gray. Asterisk: concentration of *rh1* expression.

(L) External view of the anterior prosoma of an adult male, visualized by cuticle autofluorescence.

(M) Internal view of the same specimen showing expression of *rh1* (green), *arrestin-2* (yellow), *rh3* (magenta), and nuclei in blue.

(N) Magnification of the lateral cell, expressing *arrestin-2* (yellow) and *rh3* (magenta), but not *rh1* (green).

White arrow, lateral cells; black arrowhead, median cells; white arrowhead, median eyes. Lc, lateral brain center; Oz, ozopore; L1–L2, leg 1–2. Scale bars, 100 μm (A–K), 500 μm (L and M), and 50 μm (N). See also Figure S4.

the development of the putative photoreceptors in *P. opilio*. In *Drosophila melanogaster*, *eya* and *so* are necessary for compound eye (lateral eye) and ocellus (median eye) development[41,42] and form a protein complex that works in synergy.[43] Previous work in spiders suggested that the formation of both median and lateral eye is under the control of *eya* and *so*,[25,26] and knockdown of paralog *so-A* in the spider *P. tepidariorum* affects the development of both eye types (there are no functional data for *eya* in spiders).[29] In *P. opilio*, we focused on *eya* function, given ubiquitous and early *eya* expression in the median eyes and in the early foci of expression that prefigures the location of *Po-rh1* expression in the lateral and median cells.

We conducted RNA interference (RNAi) against *Po-eya* via embryonic injections of double-stranded RNA (dsRNA). Hatchlings in the control treatment (injected with exogenous dsRNA or water) had wild-type eyes (n = 106/106) (Figure 4A). In the *Po-eya* dsRNA-injected treatment, 83% of hatchlings (n = 54/65) presented median eye defects, with a phenotypic spectrum ranging from smaller median eyes with reduced pigmentation to absence of both eyes and eye pigmentation (Figures 4B, 4C, and S5). At embryonic stages in the RNAi treatment, the eyes were smaller than in controls and showed correlated, diminished expression of *Po-eya* (Figures 4D–4F). In addition to defects in the median eyes, embryos scored as *eya* phenotypes before *in situ* hybridization also showed reduced or absent lateral and median cells, as marked by *Po-rh1* expression (n = 10/10). Notably, the degree of reduction of median eye, median cells, and lateral cells was tightly correlated, as evidenced by phenotypic mosaic individuals resulting from differential gene knockdown in cells in opposite halves of the embryo (Figure 4E). These results support a requirement for *eya* in the patterning the median eye, median cells, and lateral cells and supports the homology of median and lateral cells with eyes.

Among Chelicerata, the basally branching Pycnogonida (sea spiders) have two pairs of median eyes and no lateral eyes,[44] whereas the remaining chelicerates mostly possess both sets of visual systems, with secondary reduction of one or both eye types in miniaturized taxa.[17] Horseshoe crabs are unique in that they possess larval eyes: one pair of rudimentary lateral eyes, which becomes accessory to the compound eyes in adults, and one pair of rudimentary median eyes, which post-embryonically fuse into a subcuticular single eye accessory to

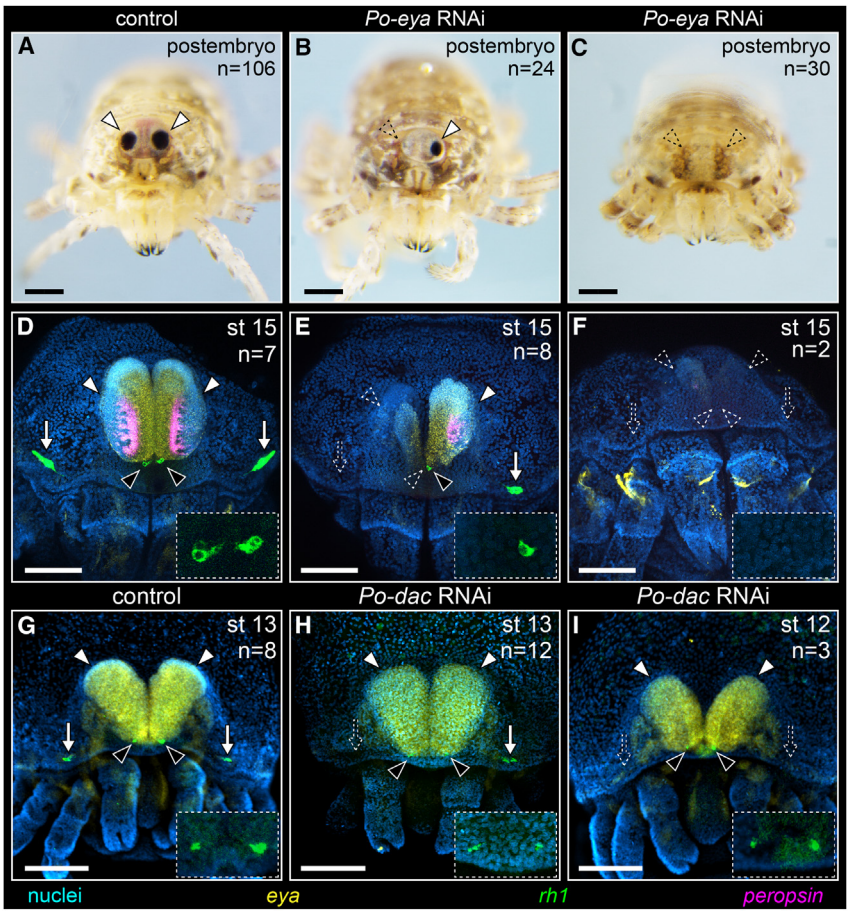

Figure 4. Median eyes and rudimentary eyes in *P. opilio* require the retinal determination network genes for normal development

(A–C) Frontal view of hatchlings in the control (A) and *eya* RNAi treatment with reduced eyes (B) and absent eyes (C).

(D–F) Frontal view of stage 15 embryos in the control (D) and *eya* RNAi treatment (E and F). *eya* (yellow), *rh1* (green), and *peropsin* (magenta) mRNA expression show the loss of both the median eyes and rudimentary eyes upon *eya* knockdown. Insets show magnification of median cells.

(G–I) Frontal view of stage 12/13 embryos in the control (G) and *dac* RNAi treatment (H and I). The *peropsin* channel was omitted.

(B), (E), and (H) are phenotypic mosaic embryos arising from differential gene knockdown in cells in opposite halves of the embryo. Nuclei in blue (Hoechst). White arrow, lateral cells; black arrowhead, median cells; white arrowhead, median eyes. Hollow, dotted arrows and arrowheads indicate loss of corresponding structures. Scale bars, 100 μm. See also Video S2 and Figure S5.

the pair of median eyes of adults.[13,39] Although the number of lateral eye pairs is variable in extant terrestrial arachnids (0–5 pairs),[17] they are thought to have a maximum of one pair of median eyes. Given the position of the median and lateral cells, we hypothesized that these putative photoreceptors of *P. opilio* are components of the median and lateral eye visual system, respectively.

To test whether the rudimentary lateral cells of *P. opilio* are serially homologous to lateral eyes of other arthropod groups (i.e., the compound eyes of pancrustaceans and horseshoe crabs), we sought a reliable marker for lateral eye identity in the literature. We initially explored *Pax2* as a potential marker of lateral eye homology, as the spider paralog *Pax2a* exhibits early expression in spider lateral eye primordia, whereas the paralog *Pax2b* is restricted to parts of the developing brain.[20] However, expression of the single-copy homolog of *Pax2* in both median eye and lateral eye primordia of *P. opilio* demonstrates that *Pax2a* is not a marker specific to chelicerate lateral eyes, as previously suggested based on expression data in two spiders[27] (supporting text at Dryad: 10.5061/dryad.m905qfv6q). Our interpretation is reinforced by data in a scorpion, wherein both paralogs of *Pax2* (the orthologs of *Pax2a* and *Pax2b* of spiders) are expressed in both median and lateral eye primordia (Figures S3F and S3G), as in the harvestman. These expression surveys suggest that the restriction of *Pax2a* to lateral eyes during eye development is a derived condition of spiders and does not reflect the dynamics of *Pax2* across Chelicerata.

As an alternative marker for lateral eye identity, we explored the retinal determination gene *dachshund* (*dac*), which is necessary for patterning lateral eyes (compound eyes) in the fruit fly *Drosophila melanogaster* and in the beetle *Tribolium castaneum* (late eye development).[30,45–47] In contrast to *eyes absent* function in both ocelli (median eyes) and compound eyes (lateral eyes), *dac* mutant fruit flies have defective compound eyes but have normal ocelli, in addition to a well-characterized deletion of medial leg segments.[45] We reasoned that if the lateral cells of *P. opilio* are serially homologous to lateral eyes, then knockdown of *Po-dac* should impair the development of the lateral cells, but not affect the development of the median eyes or median cells. We replicated an RNAi experiment against *Po-dac* and screened embryos exhibiting previously reported medial leg segment defects,[48] using the leg morphology as an indicator of successful dsRNA penetrance (Figures 4G–4I). Embryos injected with dsRNA of *Po-dac* presented wild-type median eyes and median cells but exhibited either reduction or loss of *rh1* expression in the lateral cells (n = 15/35), with a similar pattern of unilateral (mosaic) and bilateral defects, as seen in the *Po-eya* experiment (Figures 4H and 4I; Supplemental Results and Discussion). Notably, every incidence of reduction or loss of *r-opsin* in lateral cells was associated with leg axis defects on the same side, with emphasis on mosaic phenotypes.

Given the phylogenetic position of chelicerates and hexapods, these results first suggest that *dac* plays a conserved role in patterning lateral eyes across Arthropoda. However, we add the caveat that the function of *dac* homologs in the lateral eyes may vary across the phylum. For example, in the beetle *Tribolium castaneum*, maternal RNAi against *dac* does not affect the larval

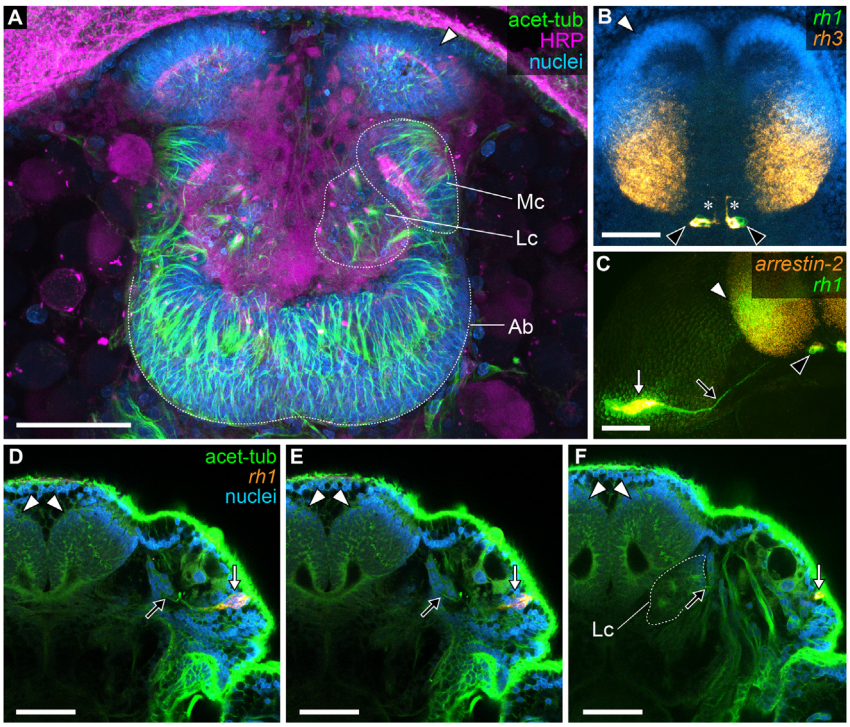

Figure 5. *P. opilio* rudimentary eyes innervate the protocerebrum

(A) Brain of a stage 14/15 *P opilio* embryo (superior view). HRP (magenta) protein marks subsets of neurons, and acetylated tubulin protein (green) is enriched in neural cells.

(B) *rh3* (uv-opsin) (orange) and *rh1* (green) mRNA (both expressed in the median cells) mark thin cellular projections (asterisks) from the median cells toward the retinal cells of the median eyes (Video S3).

(C) *arrestin-2* (orange) and *rh1* mRNA expression (green) mark cellular projections of the lateral cells toward the lateral brain center (which is positioned under the median eyes at this stage).

(D and E) Serial confocal planes of a frontal view of the embryonic head, from anterior to posterior. *rh1* mRNA expression (orange) marks the lateral cells, and acet-tub protein expression (green) shows a connection to the lateral brain center (black arrow) (Video S4). Nuclei in blue (Hoechst).

White arrow, lateral cells; black arrowhead, median cells; white arrowhead, median eyes. Ab, arcuate body; Mc, median brain center; Lc, lateral brain center. Scale bars, 50 μm.

See also Video S1 and Figure S6.

eye, whereas larval RNAi against *dac* results in reduction, but not loss, of the compound eye.[47] In the milkweed bug *Oncopeltus fasciatus*, RNAi against *dac* results in canonical loss-of-function limb phenotypes, but no eye phenotypes were reported.[49] Similarly, knockout mutants for the paralog *dac2* in the amphipod *Parhyale hawaiensis* exhibited limb phenotypes but no eye phenotypes, whereas knockouts for *dac1* exhibited no phenotype at all.[50,51] We speculate that this variation in phenotypic spectra may be attributable to the severity and penetrance of RNAi in insects and genetic compensation between paralogs in the amphipod. Alternatively, it is possible that the variation of *dac* function in lateral eye patterning may reflect developmental system drift within the RDN of Arthropoda.

Second, these results corroborate the hypothesis that median and lateral cells are part of the median and lateral eye visual systems, respectively.

P. opilio rudimentary eyes retain the protocerebral innervation pattern of separate visual systems

The median and lateral eyes of arthropods innervate distinct regions of the protocerebrum, the anterior-most component of the tripartite brain. In extant chelicerates with both median and lateral visual systems, the axons of the median eyes connect to rostral neuropils of the protocerebrum, whereas the lateral eyes connect to separate neuropils that arise from lateral domains of the protocerebrum.[13,19,34,44,52]

To establish whether the rudimentary eyes indeed exhibit phylotypic patterns of innervation, we examined neuroanatomy of the developing *P. opilio* brain. The embryonic protocerebrum of *P. opilio* (stage 15) is composed of three main regions: a rostral median center, a lateral center (ventrolateral after stage 16) that develops from the lateral furrow, and the posterior arcuate body. These three regions are recognizable by combinations of neural genes (e.g., *Po-otd* and *Po-Pax6b*; Video S1) and proteins enriched in neural cells (acetylated-tubulin; HRP) (Figures 5A and S6A–S6G). Cellular projections extending from the retinal cells of the median eyes form a nerve that projects dorsally toward the median center of the brain (Figures S6E–S6G; Video S2), in a position comparable to what has been described using cobalt and DiI/DiO retro-labeling in the eyes of adult daddy-longlegs.[19] Expression of *Po-rh1* and *Po-rh3* opsins reveals that fine cellular projections exist between the median cells and the median eye (Figures 3I and 5B; Video S3). This observation suggests that median cells and median eyes potentially share the pathway of projection into the median brain center, supporting the hypothesis that the median cells are a rudimentary pair of median eyes. Expression of photoreception-specific markers also reveals that the lateral cells project toward the lateral region of the head, adjacent to the median eyes (Figures 3B, 3E, and 5C). This projection terminates in the lateral brain center, as visualized by double-labeling of *Po-rh1* mRNA and acetylated tubulin antibody (Figures 5D–5F; Video S4). These results show that the median and lateral cells are connected to the protocerebrum in a pattern consistent with the rudimentary median and lateral eye hypothesis.

The eyes of Opiliones are not thought to be capable of sharp image formation, and the limited information on their visual ecology suggests that they function primarily as bright and dark detectors.[53,54] Reduction of eyes has been generally associated with fossorial habits and cave habitats,[55] with several examples in arachnids, including Opiliones.[29,56,57] Despite the simplified morphology of the vestigial eyes reported here, their function in immature and adult daddy-longlegs merits future investigation, with emphasis on non-image-forming functions such as

the establishment of circadian rhythms (a role associated with lateral eyes of groups like scorpions).[58,59]

Hastocularis argus, a four-eyed fossil, is a crown-group daddy-longlegs

We suspected that the previous placement of *H. argus* and *E. sheari* as stem-group Cyphophthalmi hinged upon the assumption that true lateral eyes occur only in Cyphophthalmi and true median eyes occur only in Phalangida (Figure 1A). The discovery of rudimentary lateral eyes in the daddy-longlegs *P. opilio* challenges the paradigm of absent lateral eyes in Phalangida and prompted us to reinvestigate this character and the phylogenetic placement of *H. argus*.

To test whether the rudimentary eyes we found in *P. opilio* occur more broadly across Phalangida, we collected embryos, generated genomic resources, established expression protocols, and assayed opsin expression in the armored harvestman *Iporangaia pustulosa* (a member of Laniatores, the sister group to the remaining Phalangida). Our assays unveiled that rudimentary lateral eyes occur during embryogenesis of this species as well, as demarcated by the expression of the LWS opsin *Ipus-rh1* (Figures 6C and 6D). We found no evidence of median cells in this species. Our results suggest that rudimentary lateral eyes were present in the common ancestor of daddy-longlegs (Eupnoi) and armored harvestmen (Laniatores) and, by extension, likely occur across extant Phalangida.

Next, we compiled a total-evidence dataset composed of 78 loci with minimal missing data, based on a previous phylogenomic study with well-resolved and supported relationships of the four suborders,[60] supplemented with new data for *I. pustulosa* and *Pettalus thwaitesi* (an eye-bearing Cyphophthalmi), as well as the 158 morphological characters coded in the previous analysis.[21] We first implemented the original coding in the morphological matrix (only median eyes present in Phalangida; only lateral eyes present in some Cyphophthalmi).

To infer how the presence of lateral eyes in Phalangida affects phylogenetic reconstruction, we recoded presence of lateral eyes under two schemes: (1) under strict coding, lateral eyes were scored as present in *P. opilio* (Eupnoi) and *I. pustulosa* (Laniatores), and all other Phalangida were scored as missing data for this trait; (2) under ground plan coding, lateral eyes were scored as present in all Phalangida, excepting troglobitic taxa (scored as missing data for lateral eyes). For both strict and ground plan coding, characters pertaining to median eyes were scored as unknown ("?") in all Cyphophthalmi, to reflect the unexplored possibility that mite harvestmen may retain vestiges of median eyes. The original coding scheme in our loci-rich dataset recovered *H. argus* and *E. sheari* as stem groups of Phalangida (Figure S7A), suggesting that previous inference of these taxa as stem-group Cyphophthalmi could in part have been driven by the small number of loci employed in earlier works. By contrast, both the strict and ground plan coding schemes resolved *H. argus* and *E. sheari* as nested within Eupnoi (Figures 6A, 6B, and S7B), which accords with the original description of *E. sheari* as a daddy-longlegs (Eupnoi).[61] These placements are additionally consistent with single origins of intromittent genitalia and leg elongation in the common ancestor of Phalangida (Figure S7D; supporting text at Dryad: 10.5061/dryad.m905qfv6q). As an additional test of how coding the states of eyes influences fossil placement, we coded median eyes as absent in Cyphophthalmi in the strict and ground plan matrices (i.e., as in the original matrix) but kept eye character states for Phalangida as described above. We recovered the same placement of *H. argus* and *E. sheari* within Eupnoi (Data S3 at Dryad: 10.5061/dryad.m905qfv6q).

To assess the impact of these new placements on divergence time estimation, we performed phylogenomic node dating and compared node ages with Tetraphthalmi treated as a stem-group (traditional placement) versus Tetraophthalmi treated as crown-group Eupnoi. Under the latter implementation, the median crown group of age of Eupnoi (daddy-longlegs) increased by 74 Ma compared to the original coding (344 mya versus 418 mya) (Figure S7E). The inferred ages for Phalangida and Opiliones increased by 56 and 49 Ma, respectively (Figure S7E). These results suggest that harvestmen are older than previously inferred and that crown-group Phalangida (e.g., *E. sheari*) were an established part of terrestrial Devonian ecosystems.

Vestigial eyes inform evolution of visual systems across Arthropoda

Our work provides a comprehensive molecular characterization of the median and lateral eyes of a poorly studied terrestrial chelicerate order, presenting a high-resolution atlas of multiplexed gene expression of selected regulatory genes across ontogeny and the first functional data in chelicerates for *eya* and *dac* in the context of eyes. This dataset not only precipitated the identification of two pairs of vestigial eyes in daddy-longlegs but also revealed conserved features of arthropod visual system evolution. Together with the functional evidence in the spider *P. tepidariorum* that a *sine oculis* paralog is necessary for median and eye development,[29] the evidence that *eya* (all eyes) and *dac* (lateral eyes only) have conserved functions in a chelicerate suggests that these three core components of the insect RDN patterned the visual systems of the first arthropods.

While *Pax6* paralogs in insects are early-acting genes upstream of *eya*, *so*, and *dac*,[30] a role for *Pax6* in chelicerate eyes has remained contentious[23] as no discrete early expression in the eye cells has been observed in chelicerates (but see Leite et al.[62] and discussion in Friedrich[23]). *Pax2*, a member of the Six family, had previously been suggested as a potential substitute for *Pax6*, in the specific context of spider lateral eyes.[27] Here, we showed that all Pax2 homologs are expressed in both the median and lateral eyes of a daddy-longlegs and a scorpion, suggesting that *Pax2* could play a role in both visual system eyes of chelicerates (*contra* the previously reported and spider-specific dynamics). Moreover, the early and discrete expression of *Po-Pax2* within broader domains of *Po-eya* and *Po-so* in the daddy-longlegs raises the possibility that *Pax2* may act to restrict the fate of *eya*/*so*-expressing cells in the head lobes into eye progenitor cells. Future functional investigations of *Pax2* and *Pax6* paralogs in *P. opilio* are poised to test this hypothesis.

The presence of two pairs of median eyes in the ontogeny of a daddy-longlegs (Figure 7A) also impacts inferences of ancestral number of eyes in Chelicerata. The homology of median eyes across Arthropoda, particularly with respect to the ocelli of Hexapoda and the frontal eyes of crustaceans (median eyes are absent in Myriapoda), is disputed, given variation in the number of

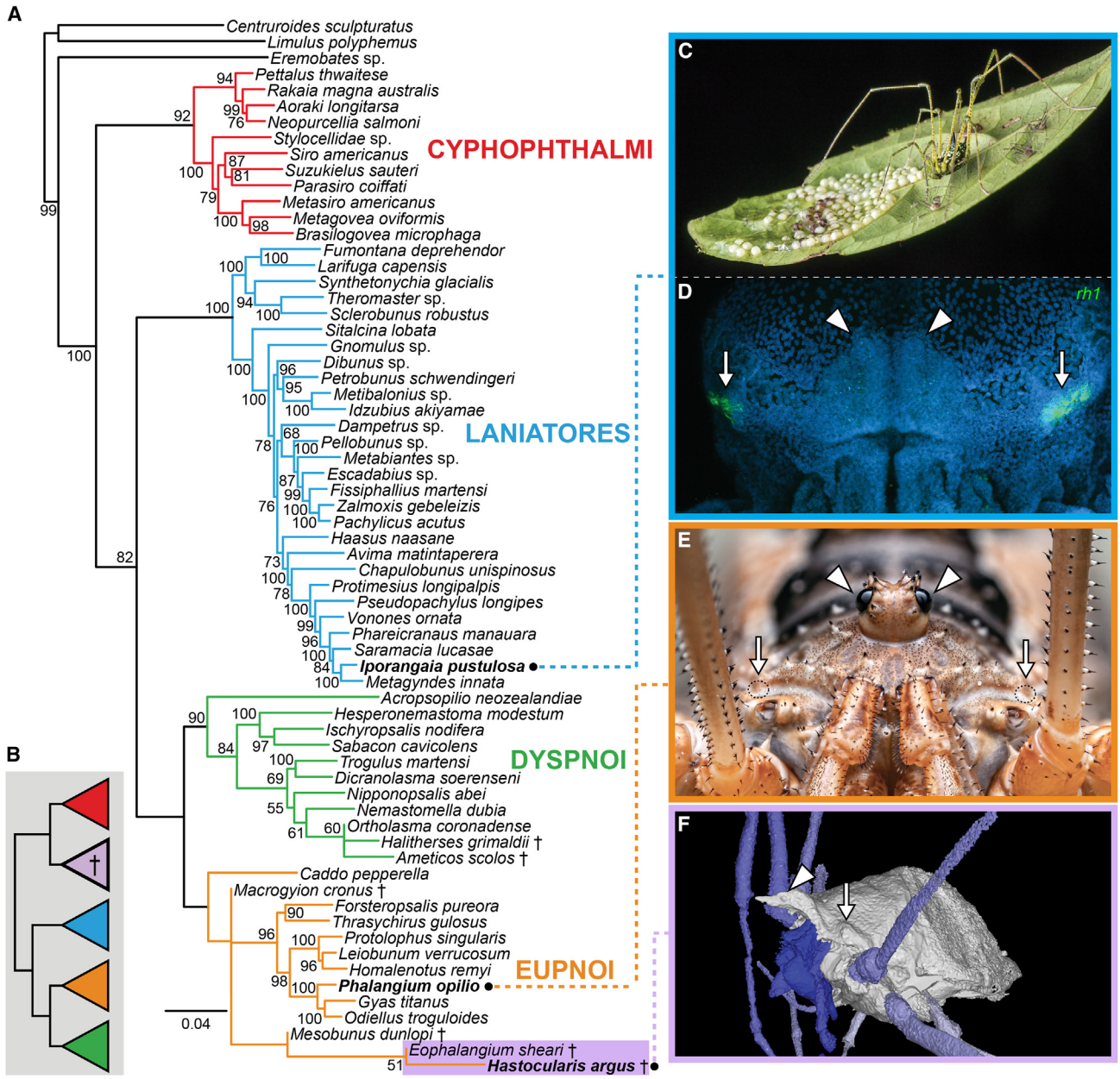

Figure 6. *Hastocularis argus*, a four-eyed fossil harvestman, is a daddy-longlegs (Eupnoi)

(A) Maximum likelihood total evidence topology of Opiliones under the strict coding scheme. Numbers on nodes are ultrafast bootstrap values (values under 50% are omitted).

(B) Schematic representation of the traditional position of *H. argus* under original coding (lateral eyes missing in Phalangida) (see also Figure S7).

(C) Male armored harvestman *Iporangaia pustulosa* guarding eggs (photo: John Uribe).

(D) *rh1* mRNA expression in the rudimentary lateral eyes of an embryo of *I. pustulosa*.

(E) Frontal view of adult female daddy-longlegs *Phalangium opilio* (photo: Roman Willi).

(F) Lateral view of *H. argus* 3D reconstruction (reproduced with permission[21]).

Arrowhead, median eye; arrow, lateral eye.

See also Figure S7.

eyes and the innervation to the protocerebrum.[14,63,64] In crustaceans, there are three conserved naupliar (larval) eyes and up to four additional frontal eyes ("frontal organs").[64] Insects typically have three dorsal ocelli,[14,65] but Collembola may have additional frontal photoreceptors.[14] On the other hand, the conserved visual pathway of the median eyes in sea spiders (Pycnogonida), horseshoe crabs (Xiphosura), and other arachnids strongly supports the homology of all median eyes across Chelicerata.[13,44,52] Nonetheless, the ancestral number of median eyes in Chelicerata is unclear, as terrestrial arachnids have a maximum of two

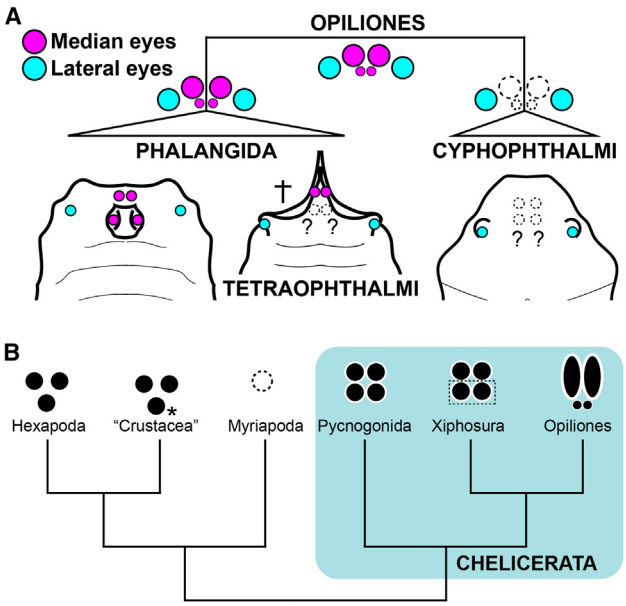

Figure 7. The implications of vestigial eyes in Opiliones

(A) Summary of Opiliones phylogeny and eye evolution with the new understanding of vestigial eyes in the context of the updated total evidence analyses. (B) Median eye condition of major arthropod lineages, with an updated understanding of median eye occurrence in Opiliones. Asterisk in Crustacea denotes the occurrence of additional frontal eyes (see Elofsson[64]). Dashed box in Xiphosura median eyes indicates fusion that occurs in late development.

median eyes, sea spiders have four, and horseshoe crabs have four median eyes embryonically (which fuse into three eyes in adults). This inference of ancestral state is further confounded by ongoing debate over the phylogenetic position of horseshoe crabs, as either sister group to the rest of the arachnids or as nested within Arachnida.[66,67] Regardless of the phylogenetic position of horseshoe crabs, the discovery of an additional pair of rudimentary median eyes in the ontogeny of daddy-longlegs, together with the condition of two median eye pairs in Pycnogonida and Xiphosura, suggests that four median eyes are part of the chelicerate ground plan (Figure 7B). This reconstruction suggests that the loss of one pair of median eyes in arachnid groups like spiders and scorpions is a derived condition, with harvestmen exhibiting an intermediate state.

Paralleling the discovery of rudimentary median eyes in *P. opilio* in this study, trilobites have recently been reported to bear three median eyes, a state comparable to many of the extant mandibulates (e.g., hexapods and crustaceans). The median eyes of trilobites are thought to have been overlooked because of their occurrence in immature stages and their subcuticular nature.[68] However, we add the caveat that the preservation of numerous arthropod fossils, as well as their rarity in many groups, is a barrier to the availability of phylogenetic data, particularly for vestigial organs that may be difficult to observe. As a specific example, the interpretation of lateral eyes in *H. argus* is predicated on (1) the presence of ozophores in this fossil and (2) the close association between ozophores and lateral eyes in mite harvestmen; there is no direct evidence of lateral eyes in Tetraophthalmi. In addition, the condition of vestigial median eyes cannot be observed in these specimens. Thus, the results reported herein for the vestigial eyes of *P. opilio* provide far more definitive data points for reconstruction of eye evolution than fossil data alone. A better understanding of median eye evolution in Chelicerata therefore requires synergy between paleontological efforts and renewed investigations of rudimentary eye ontogeny in terrestrial arachnids.

Our study documents a case where the occurrence of vestigial organs bridges a gap between past and present morphologies and underscores how vestiges in extant species can impact our understanding of fossils, phylogeny, and morphological evolution.

STAR★METHODS

Detailed methods are provided in the online version of this paper and include the following:

- KEY RESOURCES TABLE
- RESOURCE AVAILABILITY
  - Lead contact
  - Materials availability
  - Data and code availability
- EXPERIMENTAL MODEL AND SUBJECT DETAILS
  - *Phalangium opilio*
  - *Iporangaia pustulosa*, *Neosadocus maximus* and *Ampheres leucopheus*
  - *Centruroides sculpturatus*
  - *Parasteatoda tepidariorum*
- METHOD DETAILS
  - Embryo collection and fixation
  - Transcriptome sequencing and assembly
  - Gene isolation
  - RNA interference (RNAi) via double-stranded RNA (dsRNA) embryonic injections
  - *RNA interference against* Po-dac
  - Hybridization chain reaction (HCR) *in situ* hybridization and immunochemistry
  - Phylogenetic analyses and total evidence dating
- QUANTIFICATION AND STATISTICAL ANALYSIS

SUPPLEMENTAL INFORMATION

Supplemental information can be found online at https://doi.org/10.1016/j.cub.2024.02.011.

ACKNOWLEDGMENTS

We acknowledge the support of the United States National Science Foundation-Binational Science Foundation (NSF-BSF) and the National Science Foundation division of Integrative and Organismic Systems. G.G., B.C.K., P.B., E.V.W.S., and P.P.S. were supported by NSF IOS-2016141 and IOS-1552610. P.P.S. and E.G.-R. were supported by BSF-2019216 and BSF-2019823. We thank Sarah Swanson and the Newcomb Imaging Center at the botany department at the University of Wisconsin-Madison (USA) and Georg Brenneis and three anonymous reviewers for discussions and feedback on the previous drafts.

AUTHOR CONTRIBUTIONS

G.G., E.G.-R., and P.P.S. designed the scientific objectives of the study. G.G., P.P.S., B.C.K., P.B., and E.V.W.S. carried out experiments. G.G. and P.P.S. assembled transcriptomes, conducted analyses, and wrote the first

draft of the manuscript. G.G., G.P.M., and R.W. collected and preserved laniatorean harvestmen embryos. G.G. and P.P.S. created figures and tables. P.P.S. and E.G.-R. obtained funding. All of the authors contributed to the interpretation, presentation, and writing of the article and the supplemental information.

DECLARATION OF INTERESTS

The authors declare no competing interests.

Received: October 18, 2023
Revised: December 1, 2023
Accepted: February 6, 2024
Published: February 23, 2024

REFERENCES

1. Darwin, C. (1859). On the Origin of Species. (John Murray).
2. Hall, B.K. (2003). Descent with modification: the unity underlying homology and homoplasy as seen through an analysis of development and evolution. Biol. Rev. *78*, 409–433. https://doi.org/10.1017/s1464793102006097.
3. Cohn, M.J., and Tickle, C. (1999). Developmental basis of limblessness and axial patterning in snakes. Nature *399*, 474–479. https://doi.org/10.1038/20944.
4. Sutton, M.D., Briggs, D.E.G., Siveter, D.J., Siveter, D.J., and Sigwart, J.D. (2012). A Silurian armoured aplacophoran and implications for molluscan phylogeny. Nature *490*, 94–97. https://doi.org/10.1038/nature11328.
5. Luo, Z.-X., Chen, P., Li, G., and Chen, M. (2007). A new eutriconodont mammal and evolutionary development in early mammals. Nature *446*, 288–293. https://doi.org/10.1038/nature05627.
6. Müller, G. (2002). Vestigial organs and structures. In Encyclopedia of Evolution, M. Pagel, ed. (Oxford University Press).
7. Bobrovskiy, I., Hope, J.M., Ivantsov, A., Nettersheim, B.J., Hallmann, C., and Brocks, J.J. (2018). Ancient steroids establish the Ediacaran fossil *Dickinsonia* as one of the earliest animals. Science *361*, 1246–1249. https://doi.org/10.1126/science.aat7228.
8. Poschmann, M., Dunlop, J.A., Kamenz, C., and Scholtz, G. (2008). The Lower Devonian scorpion *Waeringoscorpio* and the respiratory nature of its filamentous structures, with the description of a new species from the Westerwald area, Germany. Paläontol. Z. *82*, 418–436. https://doi.org/10.1007/bf03184431.
9. Bergström, J., Stürmer, W., and Winter, G. (1980). *Palaeoisopus, Palaeopantopus* and *Palaeothea*, pycnogonid arthropods from the Lower Devonian Hunsriick Slate, West Germany. Paläontol. Z. *54*, 7–54. https://doi.org/10.1007/bf02985882.
10. Aria, C., Caron, J., and Gaines, R. (2015). A large new leanchoiliid from the Burgess Shale and the influence of inapplicable states on stem arthropod phylogeny. Palaeontology *58*, 629–660. https://doi.org/10.1111/pala.12161.
11. Henze, M.J., and Oakley, T.H. (2015). The dynamic evolutionary history of pancrustacean eyes and opsins. Integr. Comp. Biol. *55*, 830–842. https://doi.org/10.1093/icb/icv100.
12. Land, M.F. (1985). The morphology and optics of spider eyes. In Neurobiology of Arachnids (Springer-Verlag Berlin Heidelberg), pp. 53–78. https://doi.org/10.1007/978-3-642-70348-5_4.
13. Battelle, B.-A. (2006). The eyes of *Limulus polyphemus* (Xiphosura, Chelicerata) and their afferent and efferent projections. Arthropod Struct. Dev. *35*, 261–274. https://doi.org/10.1016/j.asd.2006.07.002.
14. Paulus, H.F. (1979). Eye structure and the monophyly of the Arthropoda. In Arthropod Phylogeny, A.P. Gupta, ed. (Van Nostrand Reinhold), pp. 299–383.
15. Morehouse, N.I., Buschbeck, E.K., Zurek, D.B., Steck, M., and Porter, M.L. (2017). Molecular evolution of spider vision: new opportunities, familiar players. Biol. Bull. *233*, 21–38. https://doi.org/10.1086/693977.
16. Friedrich, M. (2006). Ancient mechanisms of visual sense organ development based on comparison of the gene networks controlling larval eye, ocellus, and compound eye specification in *Drosophila*. Arthropod Struct. Dev. *35*, 357–378. https://doi.org/10.1016/j.asd.2006.08.010.
17. Miether, S.T., and Dunlop, J.A. (2016). Lateral eye evolution in the arachnids. Arachnology *17*, 103–119. https://doi.org/10.13156/arac.2006.17.2.103.
18. Shultz, J.W., and Pinto-da-Rocha, R. (2007). Morphology and functional anatomy. In Harvestmen: The Biology of Opiliones, R. Pinto-da-Rocha, G. Machado, and G. Giribet, eds. (Harvard University Press).
19. Lehmann, T., Lodde-Bensch, E., Melzer, R.R., and Metz, M. (2016). The visual system of harvestmen (Opiliones, Arachnida, Chelicerata) – a re-examination. Front. Zool. *13*. 50–16. https://doi.org/10.1186/s12983-016-0182-9.
20. Alberti, G., Lipke, E., and Giribet, G. (2008). On the ultrastructure and identity of the eyes of Cyphophthalmi based on a study of *Stylocellus* sp. (Opiliones, Stylocellidae). J. Arachnol. *36*, 379–387. https://doi.org/10.1636/csh07-120.1.
21. Garwood, R.J., Sharma, P.P., Dunlop, J.A., and Giribet, G. (2014). A Paleozoic stem group to mite harvestmen revealed through integration of phylogenetics and development. Curr. Biol. *24*, 1017–1023. https://doi.org/10.1016/j.cub.2014.03.039.
22. Sharma, P.P., and Giribet, G. (2014). A revised dated phylogeny of the arachnid order Opiliones. Front. Genet. *5*, 255. https://doi.org/10.3389/fgene.2014.00255.
23. Friedrich, M. (2022). Coming into clear sight at last: ancestral and derived events during chelicerate visual system development. Bioessays *44*, 2200163. https://doi.org/10.1002/bies.202200163.
24. Blackburn, D.C., Conley, K.W., Plachetzki, D.C., Kempler, K., Battelle, B.-A., and Brown, N.L. (2008). Isolation and expression of *Pax6* and *atonal* homologues in the American horseshoe crab, *Limulus polyphemus*. Dev. Dyn. *237*, 2209–2219. https://doi.org/10.1002/dvdy.21634.
25. Schomburg, C., Turetzek, N., Schacht, M.I., Schneider, J., Kirfel, P., Prpic, N.-M., and Posnien, N. (2015). Molecular characterization and embryonic origin of the eyes in the common house spider *Parasteatoda tepidariorum*. EvoDevo *6*, 15. https://doi.org/10.1186/s13227-015-0011-9.
26. Samadi, L., Schmid, A., and Eriksson, B.J. (2015). Differential expression of retinal determination genes in the principal and secondary eyes of *Cupiennius salei* Keyserling (1877). EvoDevo *6*, 16. https://doi.org/10.1186/s13227-015-0010-x.
27. Janeschik, M., Schacht, M.I., Platten, F., and Turetzek, N. (2022). It takes two: discovery of spider *Pax2* duplicates indicates prominent role in Chelicerate central nervous system, eye, as well as external sense organ precursor formation and diversification after neo- and subfunctionalization. Front. Ecol. Evol. *10*, https://doi.org/10.3389/fevo.2022.810077.
28. Baudouin-Gonzalez, L., Harper, A., McGregor, A.P., and Sumner-Rooney, L. (2022). Regulation of eye determination and regionalization in the spider *Parasteatoda tepidariorum*. Cells *11*, 631. https://doi.org/10.3390/cells11040631.
29. Gainett, G., Ballesteros, J.A., Kanzler, C.R., Zehms, J.T., Zern, J.M., Aharon, S., Gavish-Regev, E., and Sharma, P.P. (2020). Systemic paralogy and function of retinal determination network homologs in arachnids. BMC Genom. *21*, 811–817. https://doi.org/10.1186/s12864-020-07149-x.
30. Kumar, J.P. (2009). The molecular circuitry governing retinal determination. Biochim. Biophys. Acta *1789*, 306–314. https://doi.org/10.1016/j.bbagrm.2008.10.001.
31. Gehring, W.J. (2001). The genetic control of eye development and its implications for the evolution of the various eye-types. Zoology *104*, 171–183. https://doi.org/10.1078/0944-2006-00022.
32. Moritz, M. (1957). Zur Embryonalentwicklung der Phalangiiden (Opiliones, Palpatores) unter besonder Berücksichtigung der äußeren Morphologie, der Bildung des Mitteldarmes und der Genitalanlage. Zool. Jahrb. - Abt. Anat. Ontog. Tiere *76*, 331–370.

33. Liu, Y., Maas, A., and Waloszek, D. (2009). Early development of the anterior body region of the grey widow spider *Latrodectus geometricus* Koch, 1841 (Theridiidae, Araneae). Arthropod Struct. Dev. *38*, 401–416. https://doi.org/10.1016/j.asd.2009.04.001.

34. Doeffinger, C., Hartenstein, V., and Stollewerk, A. (2010). Compartmentalization of the precheliceral neuroectoderm in the spider *Cupiennius salei*: development of the arcuate body, optic ganglia, and mushroom body. J. Comp. Neurol. *518*, 2612–2632. https://doi.org/10.1002/cne.22355.

35. Ramirez, M.D., Pairett, A.N., Pankey, M.S., Serb, J.M., Speiser, D.I., Swafford, A.J., and Oakley, T.H. (2016). The last common ancestor of most bilaterian animals possessed at least 9 opsins. Genome Biol. Evol. *8*, 3640–3652. https://doi.org/10.1093/gbe/evw248.

36. Nagata, T., Koyanagi, M., Tsukamoto, H., Saeki, S., Isono, K., Shichida, Y., Tokunaga, F., Kinoshita, M., Arikawa, K., and Terakita, A. (2012). Depth perception from image defocus in a jumping spider. Science *335*, 469–471. https://doi.org/10.1126/science.1211667.

37. Nagata, T., Koyanagi, M., Tsukamoto, H., and Terakita, A. (2010). Identification and characterization of a protostome homologue of peropsin from a jumping spider. J Comp Physiology *196*, 51–59. https://doi.org/10.1007/s00359-009-0493-9.

38. Alvarez, C.E. (2008). On the origins of arrestin and rhodopsin. BMC Evol. Biol. *8*, 222. https://doi.org/10.1186/1471-2148-8-222.

39. Harzsch, S., Vilpoux, K., Blackburn, D.C., Platchetzki, D., Brown, N.L., Melzer, R., Kempler, K.E., and Battelle, B.A. (2006). Evolution of arthropod visual systems: development of the eyes and central visual pathways in the horseshoe crab *Limulus polyphemus* Linnaeus, 1758 (Chelicerata, Xiphosura). Dev. Dyn. *235*, 2641–2655. https://doi.org/10.1002/dvdy.20866.

40. Battelle, B.A., Dabdoub, A., Malone, M.A., Andrews, A.W., Cacciatore, C., Calman, B.G., Smith, W.C., and Payne, R. (2001). Immunocytochemical localization of opsin, visual arrestin, myosin III, and calmodulin in *Limulus* lateral eye retinular cells and ventral photoreceptors. J. Comp. Neurol. *435*, 211–225. https://doi.org/10.1002/cne.1203.

41. Bonini, N.M., Leiserson, W.M., and Benzer, S. (1993). The *eyes absent* gene: genetic control of cell survival and differentiation in the developing *Drosophila* eye. Cell *72*, 379–395. https://doi.org/10.1016/0092-8674(93)90115-7.

42. Cheyette, B.N., Green, P.J., Martin, K., Garren, H., Hartenstein, V., and Zipursky, S.L. (1994). The *Drosophila sine oculis* locus encodes a homeodomain-containing protein required for the development of the entire visual system. Neuron *12*, 977–996. https://doi.org/10.1016/0896-6273(94)90308-5.

43. Pignoni, F., Hu, B., Zavitz, K.H., Xiao, J., Garrity, P.A., and Zipursky, S.L. (1997). The eye-specification proteins So and Eya form a complex and regulate multiple steps in *Drosophila* eye development. Cell *91*, 881–891. https://doi.org/10.1016/s0092-8674(00)80480-8.

44. Brenneis, G. (2022). The visual pathway in sea spiders (Pycnogonida) displays a simple serial layout with similarities to the median eye pathway in horseshoe crabs. BMC Biol. *20*, 27. https://doi.org/10.1186/s12915-021-01212-z.

45. Mardon, G., Solomon, N.M., and Rubin, G.M. (1994). dachshund encodes a nuclear protein required for normal eye and leg development in *Drosophila*. Development *120*, 3473–3486.

46. Shen, W., and Mardon, G. (1997). Ectopic eye development in *Drosophila* induced by directed *dachshund* expression. Development *124*, 45–52. https://doi.org/10.1242/dev.124.1.45.

47. Yang, X., ZarinKamar, N., Bao, R., and Friedrich, M. (2009). Probing the *Drosophila* retinal determination gene network in Tribolium (I): The early retinal genes *dachshund*, *eyes absent* and *sine oculis*. Dev. Biol. *333*, 202–214. https://doi.org/10.1016/j.ydbio.2009.02.040.

48. Sharma, P.P., Schwager, E.E., Giribet, G., Jockusch, E.L., and Extavour, C.G. (2013). *Distal-less* and *dachshund* pattern both plesiomorphic and apomorphic structures in chelicerates: RNA interference in the harvestman *Phalangium opilio* (Opiliones). Evol. Dev. *15*, 228–242. https://doi.org/10.1111/ede.12029.

49. Angelini, D.R., and Kaufman, T.C. (2004). Functional analyses in the hemipteran *Oncopeltus fasciatus* reveal conserved and derived aspects of appendage patterning in insects. Dev. Biol. *271*, 306–321. https://doi.org/10.1016/j.ydbio.2004.04.005.

50. Bruce, H.S. (2021). How to align arthropod legs. Preprint at bioRxiv. https://doi.org/10.1101/2021.01.20.427514.

51. Bruce, H.S., and Patel, N.H. (2020). Knockout of crustacean leg patterning genes suggests that insect wings and body walls evolved from ancient leg segments. Nat. Ecol. Evol. *4*, 1703–1712. https://doi.org/10.1038/s41559-020-01349-0.

52. Lehmann, T., and Melzer, R.R. (2013). Looking like *Limulus*? – Retinula axons and visual neuropils of the median and lateral eyes of scorpions. Front. Zool. *10*, 40. https://doi.org/10.1186/1742-9994-10-40.

53. Willemart, R.H., and Giribet, G. (2010). A scanning electron microscopic survey of the cuticle in Cyphophthalmi (Arachnida, Opiliones) with the description of novel sensory and glandular structures. Zoomorphology *129*, 175–183. https://doi.org/10.1007/s00435-010-0110-z.

54. Willemart, R.H., Farine, J.-P., and Gnaspini, P. (2009). Sensory biology of Phalangida harvestmen (Arachnida, Opiliones): a review, with new morphological data on 18 species. Acta Zool. *90*, 209–227. https://doi.org/10.1111/j.1463-6395.2008.00341.x.

55. Protas, M., and Jeffery, W.R. (2012). Evolution and development in cave animals: from fish to crustaceans. WIREs Dev Biol *1*, 823–845. https://doi.org/10.1002/wdev.61.

56. Mammola, S., and Isaia, M. (2017). Spiders in caves. Proc. Biol. Sci. *284*, 20170193. https://doi.org/10.1098/rspb.2017.0193.

57. Aharon, S., Ballesteros, J.A., Crawford, A.R., Friske, K., Gainett, G., Langford, B., Santibáñez-López, C.E., Yaaran, S., Gavish-Regev, E., and Sharma, P.P. (2019). The anatomy of an unstable node: a Levantine relict precipitates phylogenomic dissolution of higher-level relationships of the armoured harvestmen (Arachnida: Opiliones: Laniatores). Invertebr. Syst. *33*, 697–717. https://doi.org/10.1071/is19002.

58. Fleissner, G., and Fleissner, G. (2003). Nonvisual photoreceptors in arthropods with emphasis on their putative role as receptors of natural Zeitgeber stimuli. Chronobiol. Int. *20*, 593–616. https://doi.org/10.1081/cbi-120023679.

59. Fleissner, G. (1977). Scorpion lateral eyes: Extremely sensitive receptors of Zeitgeber stimuli. J. Comp. Physiol. *118*, 101–108. https://doi.org/10.1007/bf00612340.

60. Fernández, R., Sharma, P.P., Tourinho, A.L., and Giribet, G. (2017). The Opiliones tree of life: shedding light on harvestmen relationships through transcriptomics. Proc. Biol. Sci. *284*, 20162340. https://doi.org/10.1098/rspb.2016.2340.

61. Dunlop, J.A., Anderson, L.I., Kerp, H., and Hass, H. (2003). Preserved organs of Devonian harvestmen. Nature *425*, 916. https://doi.org/10.1038/425916a.

62. Leite, D.J., Schönauer, A., Blakeley, G., Harper, A., Garcia-Castro, H., Baudouin-Gonzalez, L., Wang, R., Sarkis, N., Nikola, A.G., Koka, V.S.P., et al. (2022). An atlas of spider development at single-cell resolution provides new insights into arthropod embryogenesis. Preprint at bioRxiv. https://doi.org/10.1101/2022.06.09.495456.

63. Strausfeld, N.J., Ma, X., Edgecombe, G.D., Fortey, R.A., Land, M.F., Liu, Y., Cong, P., and Hou, X. (2016). Arthropod eyes: the early Cambrian fossil record and divergent evolution of visual systems. Arthropod Struct. Dev. *45*, 152–172. https://doi.org/10.1016/j.asd.2015.07.005.

64. Elofsson, R. (2006). The frontal eyes of crustaceans. Arthropod Struct. Dev. *35*, 275–291. https://doi.org/10.1016/j.asd.2006.08.004.

65. Baird, E., and Yilmaz, A. (2023). Insect dorsal ocelli: a brief overview. In Distributed Vision Springer Series in Vision Research, E. Buschbeck, and M. Bok, eds. (Springer), pp. 205–221. https://doi.org/10.1007/978-3-031-23216-9_8.

66. Ballesteros, J.A., Santibáñez-López, C.E., Baker, C.M., Benavides, L.R., Cunha, T.J., Gainett, G., Ontano, A.Z., Setton, E.V.W., Arango, C.P., Gavish-Regev, E., et al. (2022). Comprehensive species sampling and sophisticated algorithmic approaches refute the monophyly of Arachnida. Mol. Biol. Evol. *39*, msac021. https://doi.org/10.1093/molbev/msac021.

67. Lozano-Fernandez, J., Tanner, A.R., Giacomelli, M., Carton, R., Vinther, J., Edgecombe, G.D., and Pisani, D. (2019). Increasing species sampling in chelicerate genomic-scale datasets provides support for monophyly of Acari and Arachnida. Nat. Commun. *10*, 2295. https://doi.org/10.1038/s41467-019-10244-7.

68. Schoenemann, B., and Clarkson, E.N.K. (2023). The median eyes of trilobites. Sci. Rep. *13*, 3917. https://doi.org/10.1038/s41598-023-31089-7.

69. Camacho, C., Coulouris, G., Avagyan, V., Ma, N., Papadopoulos, J., Bealer, K., and Madden, T.L. (2009). BLAST+: architecture and applications. BMC Bioinf. *10*, 421. https://doi.org/10.1186/1471-2105-10-421.

70. Nguyen, L.-T., Schmidt, H.A., von Haeseler, A., and Minh, B.Q. (2015). IQ-TREE: a fast and effective stochastic algorithm for estimating maximum-likelihood phylogenies. Mol. Biol. Evol. *32*, 268–274. https://doi.org/10.1093/molbev/msu300.

71. Bryant, D.M., Johnson, K., DiTommaso, T., Tickle, T., Couger, M.B., Payzin-Dogru, D., Lee, T.J., Leigh, N.D., Kuo, T.-H., Davis, F.G., et al. (2017). A tissue-mapped axolotl de novo transcriptome enables identification of limb regeneration factors. Cell Rep. *18*, 762–776. https://doi.org/10.1016/j.celrep.2016.12.063.

72. Sievers, F., Wilm, A., Dineen, D., Gibson, T.J., Karplus, K., Li, W., Lopez, R., McWilliam, H., Remmert, M., Söding, J., et al. (2011). Fast, scalable generation of high-quality protein multiple sequence alignments using Clustal Omega. Mol. Syst. Biol. *7*, 539. https://doi.org/10.1038/msb.2011.75.

73. Edgar, R.C. (2004). MUSCLE: a multiple sequence alignment method with reduced time and space complexity. BMC Bioinf. *5*, 113. https://doi.org/10.1186/1471-2105-5-113.

74. Gouy, M., Guindon, S., and Gascuel, O. (2010). SeaView Version 4: a multiplatform graphical user interface for sequence alignment and phylogenetic tree building. Mol. Biol. Evol. *27*, 221–224. https://doi.org/10.1093/molbev/msp259.

75. Castresana, J. (2000). Selection of conserved blocks from multiple alignments for their use in phylogenetic analysis. Mol. Biol. Evol. *17*, 540–552. https://doi.org/10.1093/oxfordjournals.molbev.a026334.

76. Price, M.N., Dehal, P.S., and Arkin, A.P. (2010). FastTree 2--approximately maximum-likelihood trees for large alignments. PLoS One *5*, e9490. https://doi.org/10.1371/journal.pone.0009490.

77. Lartillot, N., Lepage, T., and Blanquart, S. (2009). PhyloBayes 3: a Bayesian software package for phylogenetic reconstruction and molecular dating. Bioinformatics *25*, 2286–2288. https://doi.org/10.1093/bioinformatics/btp368.

78. Rambaut, A., Drummond, A.J., Xie, D., Baele, G., and Suchard, M.A. (2018). Posterior summarization in bayesian phylogenetics using Tracer 1.7. Syst. Biol. *67*, 901–904. https://doi.org/10.1093/sysbio/syy032.

79. Schindelin, J., Arganda-Carreras, I., Frise, E., Kaynig, V., Longair, M., Pietzsch, T., Preibisch, S., Rueden, C., Saalfeld, S., Schmid, B., et al. (2012). Fiji: an open-source platform for biological-image analysis. Nat. Methods *9*, 676–682. https://doi.org/10.1038/nmeth.2019.

80. Gainett, G., Crawford, A.R., Klementz, B.C., So, C., Baker, C.M., Setton, E.V.W., and Sharma, P.P. (2022). Eggs to long-legs: embryonic staging of the harvestman *Phalangium opilio* (Opiliones), an emerging model arachnid. Front. Zool. *19*, 11. https://doi.org/10.1186/s12983-022-00454-z.

81. Sharma, P.P., Schwager, E.E., Extavour, C.G., and Giribet, G. (2012). Hox gene expression in the harvestman *Phalangium opilio* reveals divergent patterning of the chelicerate opisthosoma. Evol. Dev. *14*, 450–463. https://doi.org/10.1111/j.1525-142x.2012.00565.x.

82. Grabherr, M.G., Haas, B.J., Yassour, M., Levin, J.Z., Thompson, D.A., Amit, I., Adiconis, X., Fan, L., Raychowdhury, R., Zeng, Q., et al. (2011). Full-length transcriptome assembly from RNA-seq data without a reference genome. Nat. Biotechnol. *29*, 644–652. https://doi.org/10.1038/nbt.1883.

83. Sharma, P.P., Schwager, E.E., Extavour, C.G., and Giribet, G. (2012). Evolution of the chelicera: a *dachshund* domain is retained in the deutocerebral appendage of Opiliones (Arthropoda, Chelicerata). Evol. Dev. *14*, 522–533. https://doi.org/10.1111/ede.12005.

84. Gainett, G., González, V.L., Ballesteros, J.A., Setton, E.V.W., Baker, C.M., Barolo Gargiulo, L., Santibáñez-López, C.E., Coddington, J.A., and Sharma, P.P. (2021). The genome of a daddy-long-legs (Opiliones) illuminates the evolution of arachnid appendages. Proc. Biol. Sci. *288*, 20211168. https://doi.org/10.1098/rspb.2021.1168.

85. Altschul, S.F., Gish, W., Miller, W., Myers, E.W., and Lipman, D.J. (1990). Basic local alignment search tool. J. Mol. Biol. *215*, 403–410. https://doi.org/10.1016/s0022-2836(05)80360-2.

86. Battelle, B.-A., Ryan, J.F., Kempler, K.E., Saraf, S.R., Marten, C.E., Warren, W.C., Minx, P.J., Montague, M.J., Green, P.J., Schmidt, S.A., et al. (2016). Opsin repertoire and expression patterns in horseshoe crabs: evidence from the genome of *Limulus polyphemus* (Arthropoda: Chelicerata). Genome Biol. Evol. *8*, 1571–1589. https://doi.org/10.1093/gbe/evw100.

87. Smith, W.C., Greenberg, R.M., Calman, B.G., Hendrix, M.M., Hutchinson, L., Donoso, L.A., and Battelle, B.A. (1995). Isolation and expression of an arrestin cDNA from the horseshoe crab lateral eye. J. Neurochem. *64*, 1–13. https://doi.org/10.1046/j.1471-4159.1995.64010001.x.

88. Koressaar, T., and Remm, M. (2007). Enhancements and modifications of primer design program Primer3. Bioinformatics *23*, 1289–1291. https://doi.org/10.1093/bioinformatics/btm091.

89. Bruce, H.S., Jerz, G., Kelly, S.R., McCarthy, J., Pomerantz, A., Senevirathne, G., Sherrard, A., Sun, D.A., Wolff, C., and Patel, N.H. (2021). Hybridization chain reaction (HCR) in situ protocol v1 (protocols.io). https://doi.org/10.17504/protocols.io.bunznvf6.

90. Choi, H.M.T., Schwarzkopf, M., Fornace, M.E., Acharya, A., Artavanis, G., Stegmaier, J., Cunha, A., and Pierce, N.A. (2018). Third-generation in situ hybridization chain reaction: multiplexed, quantitative, sensitive, versatile, robust. Development *145*, dev165753. https://doi.org/10.1242/dev.165753.

91. Kuehn, E., Clausen, D.S., Null, R.W., Metzger, B.M., Willis, A.D., and Özpolat, B.D. (2022). Segment number threshold determines juvenile onset of germline cluster expansion in *Platynereis dumerilii*. J. Exp. Zool. B Mol. Dev. Evol. *338*, 225–240. https://doi.org/10.1002/jez.b.23100.

92. Wolfe, J.M., Daley, A.C., Legg, D.A., and Edgecombe, G.D. (2016). Fossil calibrations for the arthropod Tree of Life. Earth Sci. Rev. *160*, 43–110. https://doi.org/10.1016/j.earscirev.2016.06.008.

STAR★METHODS

KEY RESOURCES TABLE

REAGENT or RESOURCE	SOURCE	IDENTIFIER
Antibodies		
Primary: Goat polyclonal anti-HRP, Alexa Fluor 647-conjugated	Jackson ImmunoResearch Laboratories	Code: 123-605-021; RRID: AB_2338967
Primary: mouse monoclonal anti acetylated α-tubulin	Sigma-Aldrich	T6793
Secondary: goat polyclonal anti-mouse, Alexa Fluor 488-conjugated	Jackson ImmunoResearch Laboratories	Code: 115-545-003; RRID: AB_2338840
Biological samples		
Opiliones embryos and adults	Wild caught	N/A
Parasteatoda tepidariorum (Araneae)	Prashant Sharma; University of Wisconsin-Madison	N/A
Centruroides sculpturatus (Scorpiones)	Wild caught	N/A
Chemicals, peptides, and recombinant proteins		
Probe wash buffer	Molecular Instruments	N/A
Probe hybridization buffer	Molecular Instruments	N/A
Amplification buffer	Molecular Instruments	N/A
Critical commercial assays		
MEGAScript T7 kit	Thermo Fisher Scientific	AM1334
TOPO TA Cloning Kit One Shot Top 10	Thermo Fisher Scientific	K4575J10
GeneJET kit	Thermo Fisher Scientific	K0721
Deposited data		
Raw reads for the transcriptome of *Ampheres leucopheus*	This study	Genbank: SRR24709463
Raw reads for the transcriptome of *Iporangaia pustulosa*	This study	Genbank: SRR24709462
Raw reads for the transcriptome of *Neosadocus maximus*	This study	Genbank: SRR24709461
Experimental models: Organisms/strains		
Phalangium opilio	Wild caught	N/A
Ampheres leucopheus	Wild caught	N/A
Iporangaia pustulosa	Wild caught	N/A
Neosadocus maximus	Wild caught	N/A
Centruroides sculpturatus (Scorpiones)	Wild caught	N/A
Parasteatoda tepidariorum (Araneae)	Prashant Sharma; University of Wisconsin-Madison	N/A
Oligonucleotides		
Hybridization Chain Reaction *in situ* hybridization probes	Molecular Instruments and IDT	Data S1, Table S5 at Dryad: 10.5061/dryad.m905qfv6q
Software and algorithms		
BLAST+ v2.9.0+	Camacho et al.[69]	N/A
IQ-TREE v.1.6.10	Nguyen et al.[70]	N/A
TransDecoder v. 5.0.1	Bryant et al.[71]	N/A
Clustal Omega	Sievers et al.[72]	N/A
MUSCLE v.3.2	Edgar et al.[73]	N/A
Seaview v.5.0.4	Gouy et al.[74]	N/A

(*Continued on next page*)

Continued

REAGENT or RESOURCE	SOURCE	IDENTIFIER
GBlocks v.0.91b	Castresana et al.[75]	N/A
FastTree v. 2.1.10	Price et al.[76]	N/A
PhyloBayes v.3.3f	Lartillot et al.[77]	N/A
Tracer v.1.7	Rambaut et al.[78]	N/A
FIJI v.2.9.0	Schindelin et al.[79]	N/A
Photoshop 2022-2023	Adobe	N/A
Illustrator 2022-2023	Adobe	N/A

RESOURCE AVAILABILITY

Lead contact

Further information and requests for resources and reagents should be directed to and will be fulfilled by the lead contact, Guilherme Gainett (guilherme.gainett@childrens.harvard.edu).

Materials availability

This study did not generate new unique reagents.

Data and code availability

- Raw reads from bulk RNA sequencing of embryos have been deposited at NCBI and are publicly available as of the date of publication. Accession numbers are listed in the key resources table.
- All HCR probe sequences are provided in Data S1, Table S5; All raw files of confocal stacks (.czi) are available in Data S2; All the raw files for the phylogenetic analyses are available in Data S3 (Data S1–S3 are accessible in Dryad: 10.5061/dryad.m905qfv6q
- Any additional information required to reanalyze the data reported in this paper is also available from the lead contact upon request.

EXPERIMENTAL MODEL AND SUBJECT DETAILS

For all species, a range of embryonic stages was collected from multiple females on multiple days. The sex ratio for all species is presumably 50:50.

Phalangium opilio

Adult *Phalangium opilio* were collected between 2017 and 2022 in Madison, Wisconsin (USA). Animals were kept at the laboratory housed in plastic containers containing small plastic dishes with moist coconut fiber used as egg-laying surfaces. Egg clutches were kept at a 26°C incubator (VWR Gravity Convection Incubator 414005-134). Further animal care details followed protocols described previously.[80,81]

Iporangaia pustulosa, *Neosadocus maximus* and *Ampheres leucopheus*

Embryos of the laniatorean harvestmen *Iporangaia pustulosa*, *Neosadocus maximus* and *Ampheres leucopheus* (Gonyleptidae) were hand collected on January 2023 on plant leaves at State Park Intervales, Ribeirão Grande-São Paulo (Brazil) (COTEC permit #: 005416/2020-86).

Centruroides sculpturatus

Females of the scorpion *Centruroides sculpturatus* were collected from sites in Arizona (USA) by citizen-scientist collaborators and kept in the laboratory in plastic boxes until embryo harvesting.

Parasteatoda tepidariorum

Parastetoda tepidariorum individuals were obtained from a laboratory colony at the Sharma lab at Madison-Wisconsin (USA). This colony descends from colony in Cologne, Germany. Spiders were kept in plant culture tubes with a foam stoper provided with moist coconut fiber at the bottom. Cocoons with embryos were kept at room temperature for development.

METHOD DETAILS

Embryo collection and fixation

Wild type *P. opilio* embryos were collected from egg-laying dishes at the appropriate stage, following the staging in Gainett.[80] Embryos were dechorionated in commercial bleach for 15-25 min, followed by thorough washes in water and in 1x phosphate-buffered saline (PBS). Embryos used in embryonic injections were retrieved from halocarbon oil and washed with heptane for 1 min.

Embryos were fixed in scintillation vials for 1h45min in between a phase of heptane and 4% formaldehyde in 1x PBS (alternatively with a 3.2% paraldehyde solution in 1x PBS). Fixed embryos were thoroughly washed in 1x PBST (1x PBS + 0.02% Tween 20 detergent) followed by gradual dehydration into pure 180 proof ethanol (alternatively into pure methanol). Embryos were stored at -20°C for at least 1 day before use.

Embryos of the laniatorean harvestmen *I. pustulosa*, *N. maximus* and *A. leucopheus* were first cleaned in commercial bleach to remove mucus, then washed in 1x PBS profusely. For RNA sequencing, we selected a broad range of stages from embryos to post-embryo (the first stage after hatching). Embryos were fixed in RNAlater solution (Thermo Fisher, MA, USA) in the field and stored at room temperature for a week before being transferred to TRIzol (Thermo Fisher, MA, USA) and stored at -80°C until extraction. Fixation for *in situ* hybridization followed the same protocol outlined above for *P. opilio*.

Embryos of *C. sculpturatus* were dissected from gravid females in 1x PBS, fixed for 20 min in 4% formaldehyde in 1x PBS, washed in 1x PBST and gradually dehydrated into 180 proof ethanol.

Embryos of the spider *P. tepidariorum* were retrieved from cocoons and fixed in the same way as described above for *P. opilio*.

Transcriptome sequencing and assembly

Total RNA from laniatorean harvestman embryos was extracted from TRIzol fixed embryos by phase separation with BCP and precipitation with 100% isopropanol. Library preparation (TrueSeq stranded mRNA) and sequencing was performed by the Biotechnology Center of UW-Madison (USA) in an Illumina NovaSeq 6000 with a 150bp paired-read strategy. Assembly was performed with Trinity v. 2.15.1.[82]

Gene isolation

P. opilio orthologs of RDN genes *sine oculis* (*Po-so*), *Pax6a* (*Po-Pax6a*), *orthodenticle* (*Po-otd*), and *dachshund* (*Po-dac*) were previously identified from embryonic transcriptomes.[21,83] Orthologs of *eyes absent* (*Po-eya*), *Pax6b* (*Po-Pax6b*), *Pax2* (*Po-Pax2*), and *Optix* (*Po-Optix*), were identified from the *P. opilio* genome annotation.[84] All eight genes were additionally identified from either the available embryonic transcriptomes or genomic scaffolds using tblastn,[85] to cross validate their sequences and obtain the most complete transcript for downstream applications (Data S1, Table S1 at Dryad: 10.5061/dryad.m905qfv6q). The *Pax2* orthologs of the scorpion *C. sculpturatus* were identified from the genome assembly and embryonic transcriptome via tblastn using the protein sequences of the genes *Pax2a* and *Pax2b* from *P. tepidariorim* as queries. All sequences were reciprocally blasted against NCBI protein database (Data S1, Table S1 at 10.5061/dryad.m905qfv6q.

Candidate opsins were identified from the *P. opilio* genome annotation and two embryonic transcriptomes using tblastn with a protein query of the spider *P. tepidariorum* opsin sequences (seven opsins) identified by a previous study[25] (Data S1, Table S1, at Dryad: 10.5061/dryad.m905qfv6q). Candidate opsins were identified from the transcriptomes of the harvestmen *A. leucopheus*, *I. pustulosa*, *N. maximus*, and *A. acuta*, and genome annotation of the scorpion *C. sculpturatus*, via tblastn using opsin protein sequences of *P. opilio* (8 opsins) and *P. tepidariorum* as queries (Data S1, Table S2 at Dryad: 10.5061/dryad.m905qfv6q). All blast results were retrieved and subject to protein predictions with TransDecoder v. 5.0.1,[71] using a minimum length of 50 amino acids (-m 50). All proteins were aligned to a small opsin dataset from Schomburg et al.[25] with Clustal Omega[72] and a preliminary maximum likelihood analysis was performed with FastTree v.2.1.10[76] to exclude non-opsin sequences. Genes nested in the opsin clades were selected and aligned as described above to a large dataset of metazoan opsins from previous studies[15,86] and analyzed under maximum likelihood with IQ-TREE[70] (IQ-TREE v.1.6.10, *–mset LG+F+G4 –bb 1000*). Nomenclature of arachnid opsins follows Morehouse et al.[15]

P. opilio visual arrestin and myosin III orthologs were identified from the *P. opilio* genome annotation via tblastn using the horseshoe crab *Limulus polyphemus* visual arrestin (GenBank: NP_001301010.1) and myosin III (Genbank: AAC16332.3) proteins as query.[40,87] We identified one *P. opilio* ortholog of the horseshoe crab visual arrestin (*Po-arrestin-2*; ortholog of *Drosophila melanogaster Arr2*[29]), and two myosin III paralogs (*Po-myoIII-1*; *Po-myoIII-2*) (Data S1, Table S1 at Dryad: 10.5061/dryad.m905qfv6q).

RNA interference (RNAi) via double-stranded RNA (dsRNA) embryonic injections

A 921 bp fragment of *Po-eya* spanning part of the coding sequence was amplified from a cDNA library using gene-specific primers designed with Primer3 v. 4.1.0[88] and appended with T7 ends. This fragment was linked to a plasmid vector into competent *Escherichia coli* with the TOPO TA Cloning Kit One Shot Top 10 (Thermo Fisher, MA, USA) following the standard protocol. Plasmids were purified with a GeneJET kit (Thermo Fisher, MA, USA) and sanger sequenced for verification (Data S1, Table S3 at Dryad: 10.5061/dryad.m905qfv6q).

dsRNA was synthetized with the MEGAScript T7 kit (Thermo Fisher, MA, USA). Two clutches of embryos (n = 608 embryos) were used for *Po-eya* dsRNA (knockdown; n = 448) and vector dsRNA (control; n = 160) embryonic injections (Figure S5).

Embryos were affixed to plastic cover slips with heptane glue, and injected under Halocarbon 700 oil (Sigma-Aldrich, MO, USA) with a micromanipulator (MMO-202ND, Narishige, Tokyo, Japan) and microinjection unit (IM 300, Narishige). Needles were pulled

from borosilicate glass capillaries (World Precision Instruments 1B100F-4) with a Sutter Instruments P-1000 micropipette puller. Injection volume was prepared with rhodamine dextran (1:20) for visualization, at a final concentration between 4 and 4.5 μg/μL. The experiment was replicated in five additional clutches (*Po-eya* dsRNA; dH_20 control), which were fixed and exclusively used in fluorescent *in situ* hybridization. Clutches of embryos were injected between stage 5 (germ disc) and stage 8, which is before the beginning of the head ectoderm folding process that forms the brain and the eyes. Hatchlings from treatment and control experiments were sorted into four categories of phenotypes: wild type; both eyes lost; one eye small, other eye lost; both eyes small; one eye small, other eye wild type. Only embryos that hatched or nearly hatched (stages 18, 19) were considered in the counts.

RNA interference against Po-dac

Experimental design, primers and cloned fragment followed a previous study of *dac* function in *P. opilio* leg development.[48] To test the serial homology of the lateral cells as rudiments of lateral eyes (e.g., the facetted eyes of pancrustaceans and horseshoe crabs) we performed RNAi against *Po-dac*. This experiment was predicated on the observation that the loss-of-function mutant of *dac* in the fruit fly *D. melanogaster* exhibits defects or loss of the lateral eyes (compound eyes), but shows no effect on the ocelli (median eyes).

Of 200 embryos injected with *Po-dac* dsRNA, 35 embryos were selected that exhibited unilateral (mosaic) or bilaterally symmetrical leg defects. These embryos were assayed for *rh1* and *eya* expression; 26 embryos were fixed four days after injection (ca. stage 12-13) and another 9 embryos were fixed six days after injection (ca. stage 15 or older). Of the 26 embryos fixed at stages 12-13, we observed bilaterally symmetrical absence of *rh1* in lateral cells (n = 3), absence of *rh1* expression in lateral cells on one side only (n = 5), reduction of *rh1* in lateral cells on one side only (n = 5), or wild type expression (n = 8). In embryos exhibiting reduction or loss of *rh1* expression in lateral cells, the affected side also exhibited canonical *dac* loss-of-function phenotypes in the appendages (truncation or fusion of medial leg segments). The remaining five embryos could not be assayed for *rh1* expression (fixed too early or insufficient signal for phenotyping). Of the 9 embryos fixed at stages 15 or older, we observed reduction of *rh1* expression in lateral cells on one side only (n = 2), or wild type expression (n = 6). The remaining one embryo could not be assayed for *rh1* expression (insufficient signal for phenotyping). Notably, loss of *rh1* was never observed in the median cells (rudimentary median eyes), suggesting that the effect of *dac* RNAi is specific to the lateral cells.

Of the 20 embryos injected with exogenous dsRNA (negative controls), 9 were assayed for *rh1* and *eya* expression. Wild type expression of *rh1* and *eya* was observed in 8/9 embryos.

Hybridization chain reaction (HCR) *in situ* hybridization and immunochemistry

Hybridization Chain Reaction (HCR) *in situ* hybridization followed a modified version of the Molecular Instruments (Los Angeles, CA, USA) hybridization chain reaction (HCR) v.3 protocol.[89,90] Probe sequences were designed and synthesized by Molecular Instruments or in an open-source software[91] and ordered from IDT (USA). Probe catalog numbers, sequences and details about initiators are available in Data S1, Table S5 at Dryad: 10.5061/dryad.m905qfv6q. Combined HCR and immunochemistry staining followed the protocol in.[80,89] The following antibodies were used: (1) primary antibody: goat anti-HRP (123-605-021; Jackson ImmunoResearch Laboratories); (2) primary antibody: mouse acetylated α-tubulin (T6793; Sigma-Aldrich) at 1:500 dilution; (3) secondary antibody: goat anti-mouse Alexa Fluor 488-conjugated (115-545-003; Jackson ImmunoResearch Laboratories) at 1:200 dilution. Imaging was performed on a Zeiss 710 and Zeiss 780 confocal microscope at the Newcomb Imaging Center, UW-Madison, USA. Unless otherwise noted, fluorescent microscopy images are maximum intensity projections, which were linearly adjusted for brightness and contrast in FIJI (v. 2.9.0/1.53t) avoiding overexposure of pixels. Brightfield images were obtained on a Nikon SMZ25 fluorescent stereomicroscope with a DS-Fi2 digital color camera driven by Nikon Elements software. Plates were assembled in Adobe Illustrator 2022.

Phylogenetic analyses and total evidence dating

Total evidence phylogenetic analysis was performed by combining a previously established taxon 78-gene phylotranscriptomic dataset with minimal missing data[60] with a matrix consisting of 158 morphological characters.[21] To facilitate placement of phylogenetically significant taxa in this study, new sequences were added for *P. thwaitesi* (Genbank: SRR9611071) or retrieved from the embryonic transcriptome of *I. pustulosa* (Genbank: SRR24709462) via blastn searches, followed by multiple sequence alignment with MUSCLE v.3.2[73] and trimming of overhanging ends with GBlocks v.0.91b.[75] *I. pustulosa* was coded for all 158 morphological characters in the matrix. The complete dataset consisted of 60 extant and six fossil taxa. Outgroups consisted of the horseshoe crab *L. polyphemus*, the scorpion *C. sculpturatus*, and the solifuge *Eremobates* sp.

Three alternative morphological coding schemes were implemented. In the first matrix (original coding), reflecting the traditional understanding of harvestman eye evolution, lateral eyes were coded as present only in two groups of Cyphophthalmi (Stylocellidae and Pettalidae) and median eyes were coded as present only in Phalangida (except for troglobitic species, which were scored as absent for all eyes).

Next, we generated two new matrices with updated coding of the character ‘‘Lateral eyes’’ to reflect the presence of rudimentary eyes discovered in this work. We interpret the presence of rudimentary lateral eyes in a broad sense that avoids discriminating between larval and adult lateral eyes, in light of the understanding that in other arthropods these are thought to be parts of the same developmental field.[16]

In the second matrix (strict coding), lateral eyes (character 3) were coded as present (state 0) in *P. opilio* and *I. pustulosa*, and as missing data (?) in all other Phalangida; the number of lateral eye pairs (character 4) were coded as one pair (state 4) in *P. opilio* and *I. pustulosa*, and as missing data (?) in all other Phalangida; and the condition of the lateral eye rhabdomes was scored as unknown (?)

in all Phalangida. In the third matrix (ground plan coding), given that the common ancestor of *P. opilio* and *I. pustulosa* is equivalent to the common ancestor of all Phalangida, we trialed scored all non-troglobitic Phalangida as bearing a single pair of lateral eyes, with an unknown condition of the lateral eye rhabdomes. The ground plan coding was performed to assess how the potential discovery of lateral eyes in other groups of Phalangida would affect the analysis (and specifically, nodal support values), toward addressing the possibility that missing data for lateral eye condition may be driving the results obtained in this study.

Median eyes were coded as missing data ("?") for all Cyphophthalmi for both the strict and ground plan coding matrices; given the unexpected discovery of rudimentary median eyes in Phalangida, we consider the presence of undiscovered rudimentary median eyes in Cyphophthalmi to be an unexplored possibility. Nevertheless, we also performed a separate family of analyses, coding median eyes as absent for all Cyphophthalmi, to assess whether the traditional understanding of eye incidence in this group influences phylogenetic positions of fossils. Lastly, we performed one additional pair of analyses (strict and ground plan coding) with a new character describing the degree of lateral eye regression (present in *P. opilio* and *I. pustulosa*). The matrices are available in Data S3 at Dryad: 10.5061/dryad.m905qfv6q.

Maximum likelihood analyses were conducted with IQ-TREE v.2,[70] with six partitions (morphology and five loci). Best-fitting one-parameter Markov and LG + I + G models were inferred for the single morphological and 78 molecular data partitions, respectively. Nodal support was inferred using 1000 ultrafast bootstrap resampling replicates.

Phylogenomic divergence time estimation was performed using PhyloBayes v.3.3f.[77] A constraint tree was provided, based on maximum likelihood analyses of the molecular dataset, and placing the root between Opiliones + Solifugae and Scorpiones + Xiphosura. The rooting reflects recent inferences of higher level chelicerate relationships.[66] To compare the effect of Tetraophthalmi placement (stem-group Cyphophthalmi *sensu* Garwood et al.[21] versus crown group Eupnoi), we implemented two sets of node calibrations. In the Tetraophthalmi stem-group calibration strategy, we calibrated the basal split of Opiliones with a floor of 411 Myr (based on the Devonian fossil *E. sheari*), and both Eupnoi and Dyspnoi with a floor of 305 Myr (based on the Carboniferous fossils *Macrogyion cronus* and *Ameticos scolos*, respectively). In the Tetraophthalmi as crown group Eupnoi calibration strategy, we calibrated the crown age of Eupnoi with a floor of 411 Myr, the crown age of Dyspnoi with a floor of 305 Myr, and did not calibrate the basal split of Opiliones. Three other node calibrations (root age, split between scorpions and horseshoe crabs, and minimum age of Cyphophthami) were used identically for both analyses and are based on a recent compendium of fossils for node calibrations across arthropods.[92] For both analyses, a CAT-GTR substitution model and a lognormal clock model were implemented. Three chains were run for several thousand generations for each calibration strategy and the first ten thousand cycles were discarded as burnin after assessment of chain mixing with Tracer v.1.7[78] (Data S3 at Dryad: 10.5061/dryad.m905qfv6q). Fossil calibrations and justifications are provided in Data S1, Table S4 at Dryad: 10.5061/dryad.m905qfv6q.

QUANTIFICATION AND STATISTICAL ANALYSIS

Quantification of embryonic phenotypes is explained in method details. "n" indicates the number of individuals assessed. No statistical tests were conducted to compare treatments. Methods for phylogenetic and dating analyzes are explained in method details.